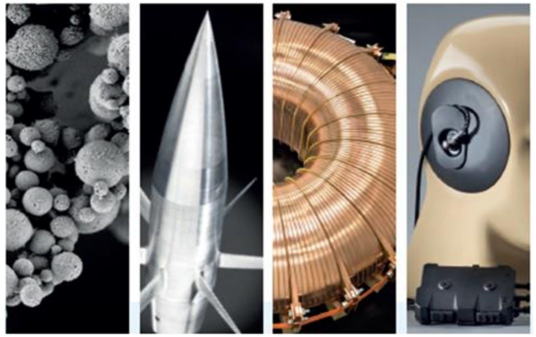

[1] ISL - French-German Research Institute of Saint-Louis
[2] University Grenoble Alpes, Grenoble INP, GIPSA-lab

Flight Dynamics Modeling for Long-Range Guided Projectiles (LRGP)

Gian Marco VINCO [1][2]

7th October 2021

Supervisors

Prof. Olivier SENAME [2]
Dr. Spilios THEODOULIS [1]

A joint initiative of

AGENCE INNOVATION DÉFENSE

MINISTÈRE DES ARMÉES

Bundesministerium der Verteidigung

Project Overview

Study of a new *Long-Range Guided Projectile* (LRGP) concept.

Development of a full 6DOF nonlinear guided simulator environment.

Static aerodynamic characterization, and derivation of a new aerodynamics model for the LRGP concept.

Design of the pitch and the roll autopilots by employing the *Linear Parameter Varying* (LPV) approach.

Performance and control robustness properties assessment.

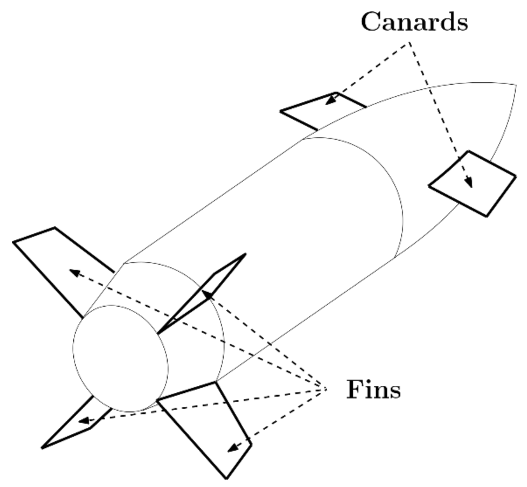

Figure 1.
LRGP concept: emphasis on the aerodynamic surfaces.

CFD Simulation Measurements

- The static characterization of the projectile aerodynamics was performed by means of *Computational Fluid Dynamics* (CFD) software simulations.
- The static measurements were provided in the form of aerodynamic forces (X, Y, Z) and moments (L, M, N), coherent with the body reference system of coordinates (B), as in Figure 2.
- These measurements were normalized with respect to the dimensions of the projectile and expressed as non-dimensional static coefficients (C_{X_s}, C_{Y_s}, C_{Z_s}) and (C_{l_s}, C_{m_s}, C_{n_s}), respectively.
- Each coefficient was first measured in accordance with a polar system of coordinates, as a function of the *Mach number* (M), the *roll angle* (ϕ') and the *total angle-of-attack* (α'), more suitable for the CFD software.
- Then, the measurements were converted to the Cartesian system of coordinates, as a function of the *angle-of-attack* (α) and *angle-of-sideslip* (β), more suitable for modeling and control design purposes.

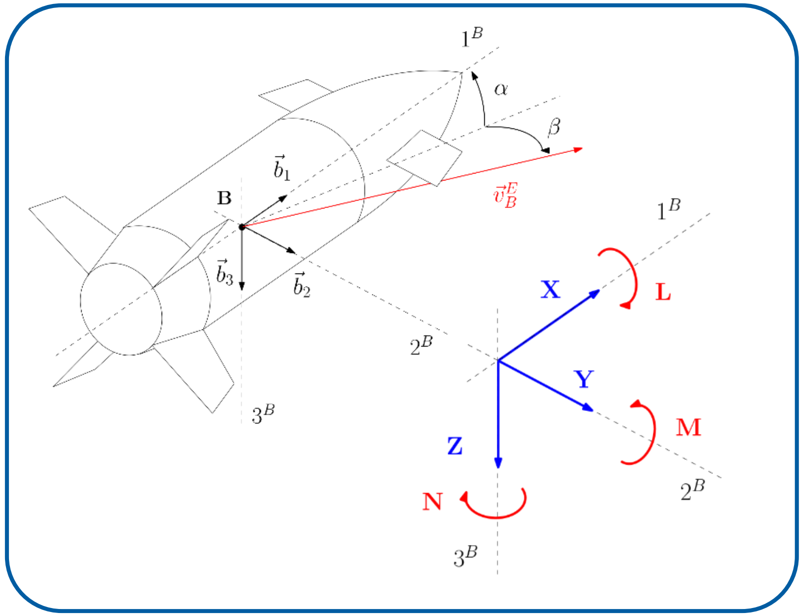

Figure 2. Body reference system, and main aerodynamic measurements.

Polar Coordinates ⟺ Cartesian Coordinates

$$\begin{cases} \alpha' = \arccos(\cos\alpha\cos\beta) \\ \phi' = \arctan\left(\dfrac{\tan\beta}{\sin\alpha}\right) \end{cases} \qquad \begin{cases} \alpha = \arctan(\tan\alpha'\cos\phi') \\ \beta = \arcsin(\sin\alpha'\sin\phi') \end{cases}$$

Equation 1. Aerodynamic coordinates relations.

Investigated Regression Approaches

For each Mach value in the range $[M_{\text{min}}, \dots, M_{\text{max}}]$, a roll angle ϕ' was selected $[0, \dots, 90]$ [deg]. Then, the data were acquired by varying the total angle-of-attack in the range $[0, \dots, \alpha'_{\text{max}}]$ [deg].

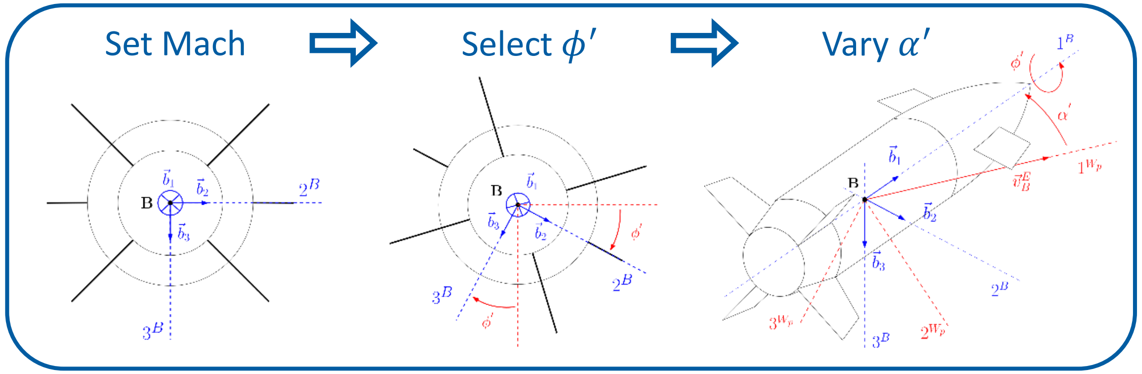

Figure 3. CFD Measurements acquisition procedure.

As in Equation 1, if $\phi' = 0$ [deg], then $\alpha' = \alpha$; if $\phi' = 90$ [deg], then $\alpha' = \beta$. Thus, the converted aerodynamic measurements are expressed as a function of either α or β (*Reduced CFD dataset*).

For intermediate values of the roll angle, the converted aerodynamic measurements are expressed as a function of the simultaneous variation of the angles α and β (*Full CFD dataset*).

	Simple Linear Regression	Multivariable Regression
CFD dataset	➢ Reduced set of CFD measurements neglecting the simultaneous variations of multiple variables.	➢ Full set of CFD measurements modeling the combined effects generated by the variations of α and β.
Regression Methods	➢ Standard polynomial regression [1]. ➢ Least-squares optimization.	➢ Multivariable regression. ➢ Least-squares optimization.
Advantages	✓ Simplified mathematical model. ✓ Literature background.	✓ Higher model accuracy across the entire flight envelope. ✓ Physical coherency.
Limits	X Lower accuracy deriving from the model approximations.	X Higher complexity level of the mathematical model because of the inclusion of bilinear terms.

Table 1. Regression approaches comparison chart.

NB: All the presented data have been rescaled for confidentiality reasons.

[1] Zipfel, P. (2014). *Modeling and simulation of aerospace vehicle dynamics*. American Institute of Aeronautics and Astronautics.

Simple Linear Regression

- Based on the standard polynomial regression approach, and on the least-squares optimization.
- Several polynomial functions of increasing odd or even order were investigated for each coefficient regression, modeling the variation of either α or β.
- The model accuracy was assessed in terms of the *Sum of Squared Errors* (SSE), *Coefficient of Determination* (R^2), *Root Mean Squared Error* (RMSE), statistical coefficients, as shown in Figure 4.

$$\begin{cases} C_{X_s}(M,\alpha) = C_{X_{\alpha 0}}(M) + C_{X_{\alpha 2}}(M)\sin^2\alpha \\ C_{X_s}(M,\alpha) = C_{X_{\alpha 0}}(M) + C_{X_{\alpha 2}}(M)\sin^2\alpha + C_{X_{\alpha 4}}(M)\sin^4\alpha + \dots \end{cases}$$

$$\begin{cases} C_{Y_s}(M,\beta) = C_{Y_{\beta 1}}(M)\sin\beta \\ C_{Y_s}(M,\beta) = C_{Y_{\beta 1}}(M)\sin\beta + C_{Y_{\beta 1}}(M)\sin^3\beta + \dots \end{cases}$$

Equation 2. Polynomial regression functions examples.

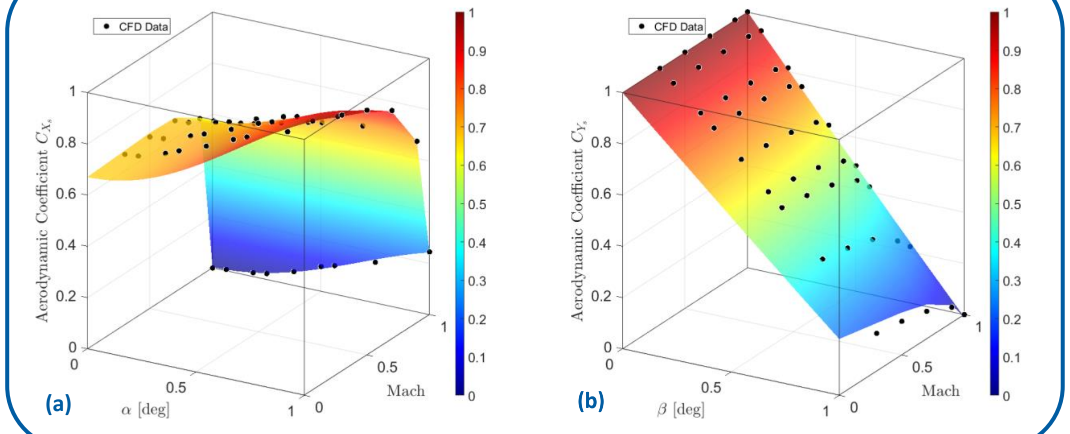

Figure 5. Resulting regression surfaces: longitudinal (a) and lateral (b) forces.

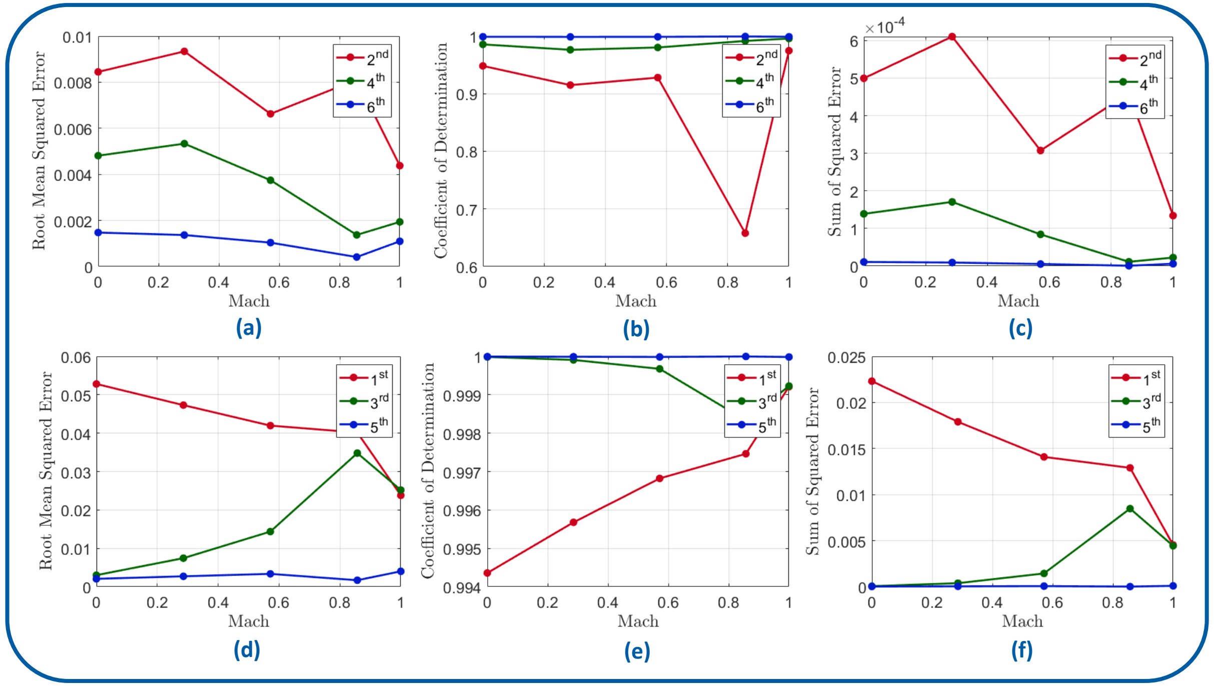

Figure 4. Regression accuracy analysis: RMSE, R^2, and SSE, respectively for the longitudinal ((a),(b),(c)) and the lateral ((d),(e),(e)) forces.

NB: All the presented data have been rescaled for confidentiality reasons.

Simple Linear Regression

	Polynomial Order	SSE	R^2	RMSE
$C_{X_\alpha}(M,\alpha)$	2nd 4th	$0.4 \cdot 10^{-3}$ $0.1 \cdot 10^{-3}$	85% 98%	$0.7 \cdot 10^{-2}$ $0.3 \cdot 10^{-2}$
$C_{Y_\alpha}(M,\alpha)$	3rd 5th	$0.2 \cdot 10^{-5}$ $0.1 \cdot 10^{-6}$	75% 98%	$0.4 \cdot 10^{-3}$ $0.1 \cdot 10^{-3}$
$C_{Z_\alpha}(M,\alpha)$	1st 3rd	$0.5 \cdot 10^{-4}$ $0.4 \cdot 10^{-4}$	99% 99%	$0.2 \cdot 10^{-1}$ $0.2 \cdot 10^{-1}$
$C_{l_\alpha}(M,\alpha)$	3rd 5th	$0.6 \cdot 10^{-6}$ $0.3 \cdot 10^{-6}$	50% 70%	$0.3 \cdot 10^{-3}$ $0.3 \cdot 10^{-3}$
$C_{m_\alpha}(M,\alpha)$	3rd 5th	$0.3 \cdot 10^{-1}$ $0.1 \cdot 10^{-1}$	87% 96%	$0.7 \cdot 10^{-1}$ $0.4 \cdot 10^{-1}$
$C_{n_\alpha}(M,\alpha)$	1st 3rd	$0.2 \cdot 10^{-4}$ $0.6 \cdot 10^{-5}$	50% 80%	$1 \cdot 10^{-3}$ $0.5 \cdot 10^{-3}$

Table 2. Accuracy results related to the α coefficient derivatives.

	Polynomial Order	SSE	R^2	RMSE
$C_{X_\beta}(M,\beta)$	2nd 4th	$0.9 \cdot 10^{-3}$ $0.1 \cdot 10^{-3}$	80% 99%	$0.1 \cdot 10^{-1}$ $0.4 \cdot 10^{-2}$
$C_{Y_\beta}(M,\beta)$	1st 3rd	$0.2 \cdot 10^{-1}$ $0.4 \cdot 10^{-2}$	99% 99%	$0.4 \cdot 10^{-1}$ $0.2 \cdot 10^{-1}$
$C_{Z_\beta}(M,\beta)$	1st 3rd	$0.4 \cdot 10^{-6}$ $0.1 \cdot 10^{-6}$	50% 87%	$0.2 \cdot 10^{-3}$ $0.1 \cdot 10^{-3}$
$C_{l_\beta}(M,\beta)$	3rd 5th	$0.9 \cdot 10^{-7}$ $0.6 \cdot 10^{-7}$	60% 70%	$0.1 \cdot 10^{-3}$ $0.9 \cdot 10^{-4}$
$C_{m_\beta}(M,\beta)$	1st 3rd	$0.2 \cdot 10^{-5}$ $0.1 \cdot 10^{-5}$	50% 70%	$0.5 \cdot 10^{-3}$ $0.4 \cdot 10^{-3}$
$C_{n_\beta}(M,\beta)$	1st 3rd	$0.5 \cdot 10^{-1}$ $0.2 \cdot 10^{-1}$	98% 99%	$0.8 \cdot 10^{-1}$ $0.4 \cdot 10^{-1}$

Table 3. Accuracy results related to the β coefficient derivatives.

Only the relevant coefficient derivatives are included in the final model, while minor terms are neglected. The roll coefficient C_{l_s} is ignored in the model since both the derivatives are negligible.

$$\begin{cases} C_{X_s}(M,\alpha) = C_{X_{\alpha 0}}(M) + C_{X_{\alpha 2}}(M)\sin^2\alpha + C_{X_{\alpha 4}}(M)\sin^4\alpha \\ C_{Y_s}(M,\beta) = C_{Y_{\beta 1}}(M)\sin\beta \\ C_{Z_s}(M,\alpha) = C_{Z_{\alpha 1}}(M)\sin\alpha \\ C_{m_s}(M,\alpha) = C_{m_{\alpha 1}}(M)\sin\alpha + C_{m_{\alpha 3}}(M)\sin^3\alpha + C_{m_{\alpha 5}}(M)\sin^5\alpha \\ C_{n_s}(M,\beta) = C_{n_{\beta 1}}(M)\sin\beta \end{cases}$$

Equation 3. Full *Simple Linear Regression* model.

Based on a *Multivariable Regression* approach, aiming to model the coupled effects generated by the simultaneous α and β variations.

Several multivariable functions were investigated: for each coefficient, a *Test function*, a *Formula function,* and an *Independent function* were considered.

The model accuracy was assessed in terms of the *Sum of Squared Errors* (SSE), *Coefficient of Determination* (R^2), *Root Mean Squared Error* (RMSE), statistical coefficients, as shown in Figure 6.

Test: selected as the most accurate model among a large set of trial functions, aiming to best fit the CFD data.

Formula: based on flight mechanics theoretical derivations [1].

Independent: assuming each individual regression parameter to be a function of either α or β.

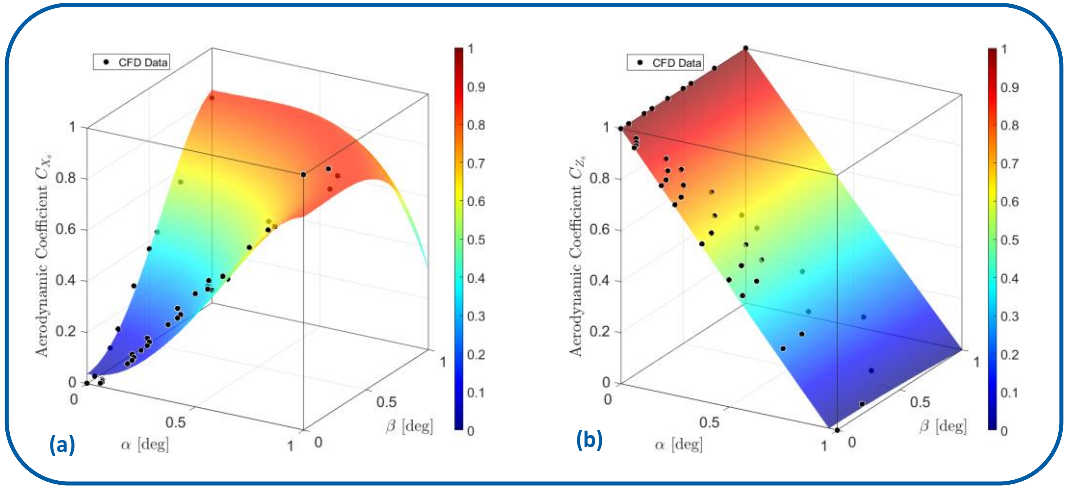

Figure 7. Resulting regression surfaces: longitudinal (a) and vertical (b) forces.

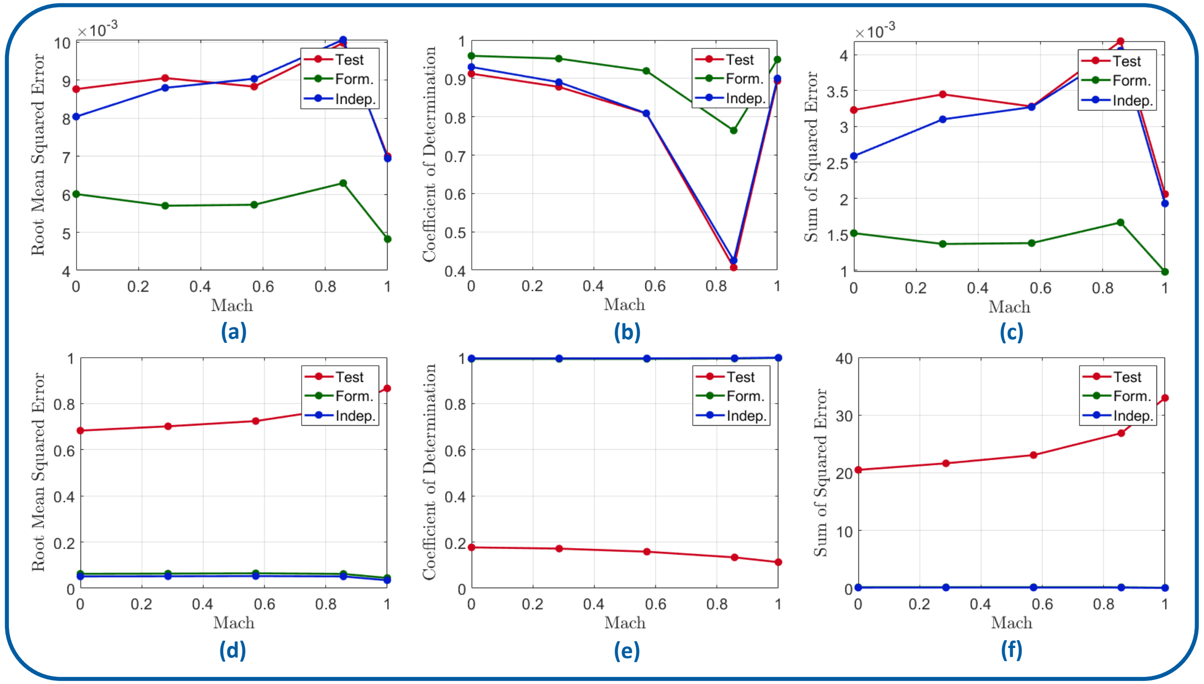

Figure 6. Regression accuracy analysis: RMSE, R^2, and SSE, respectively for the longitudinal ((a),(b),(c)) and the vertical ((d),(e),(f)) forces.

[1] McCoy, R. (1999). *Modern exterior ballistics: the launch and flight dynamics of symmetric projectiles,* Schiffer.

- Because of the coherency with the flight mechanics formulation, and the results obtained in terms of model accuracy, the Formula model was employed for the final comparison.
- As observed for the Simple Linear Regression, the roll coefficient C_{l_s} derivatives are negligible, thus it is ignored in the model.

$$
\begin{cases}
C_{X_s}(M,\alpha,\beta) = C_{X_0}(M) + C_{X_2}(M)\cos\alpha\cos\beta + C_{X_4}(M)\cos^2\alpha\cos^2\beta \\
C_{Y_s}(M,\alpha,\beta) = C_{Y_2}(M)\sin\beta\cos\alpha \\
C_{Z_s}(M,\alpha,\beta) = C_{Z_2}(M)\sin\alpha\cos\beta \\
C_{m_s}(M,\alpha,\beta) = C_{m_2}(M)\sin\alpha\cos\beta + C_{m_4}(M)\sin\alpha\cos\alpha\cos^2\beta \\
C_{n_s}(M,\alpha,\beta) = C_{n_2}(M)\sin\beta\cos\alpha
\end{cases}
$$

Equation 4. Full *Multivariable Regression* model.

	Regression Model	SSE	R^2	RMSE
$C_{X_s}(M,\alpha,\beta)$	Test	$0.2\cdot10^{-2}$	85%	$0.8\cdot10^{-2}$
	Formula	$0.1\cdot10^{-2}$	92%	$0.6\cdot10^{-2}$
	Independent	$0.2\cdot10^{-2}$	75%	$0.9\cdot10^{-2}$
$C_{Y_s}(M,\alpha,\beta)$	Test	$0.4\cdot10^{-1}$	99%	$0.4\cdot10^{-1}$
	Formula	$0.4\cdot10^{-1}$	99%	$0.3\cdot10^{-1}$
	Independent	$0.3\cdot10^{-1}$	99%	$0.2\cdot10^{-1}$
$C_{Z_s}(M,\alpha,\beta)$	Test	$0.6\cdot10^{-1}$	99%	$0.4\cdot10^{-1}$
	Formula	$0.5\cdot10^{-1}$	99%	$0.4\cdot10^{-1}$
	Independent	$0.4\cdot10^{-1}$	99%	$0.3\cdot10^{-1}$
$C_{m_s}(M,\alpha,\beta)$	Test	0.2	70%	0.8
	Formula	0.1	85%	0.6
	Independent	0.2	75%	0.8
$C_{n_s}(M,\alpha,\beta)$	Test	0.15	98%	$0.6\cdot10^{-1}$
	Formula	0.12	98%	$0.5\cdot10^{-1}$
	Independent	0.12	98%	$0.5\cdot10^{-1}$

Table 4. Accuracy results related to the multivariable coefficient derivatives.

Model Comparison

Since the *Multivariable* and the *Simple Linear Regression Models* are derived from different datasets, the previous statistical results do NOT allow a direct comparison of the two approaches.

⇨ Additional interpolation error comparison across the analyzed flight envelope (α', ϕ', M).

Error Analysis Algorithm

$for\ \phi'$
  $for\ M$
    $for\ \alpha'$
      $\alpha, \beta = f(\alpha', \phi')$

      CFD Data Interpolation -------------------
      $C_{\mathrm{CFD}_i} = interp(\alpha', M)$

      Multivariable Interpolation --------------
      $C_1, C_2, \ldots = interp(M)$
      $C_{\mathrm{M}_i} = C_1 f(\alpha, \beta) + C_2 f(\alpha, \beta) \ldots$

      Simple Linear Interpolation -------------
      $C_1, C_2, \ldots = interp(M)$
      $C_{\mathrm{S}_i} = C_1 f(\alpha\ or\ \beta) + C_2 f(\alpha\ or\ \beta) \ldots$

    end
  end
end

e_{M_i} ; e_{S_i}

3D $(n \times m \times l)$ error data tables.

where,

n : length of α' dataset
m : length of M dataset
l : length of ϕ' dataset

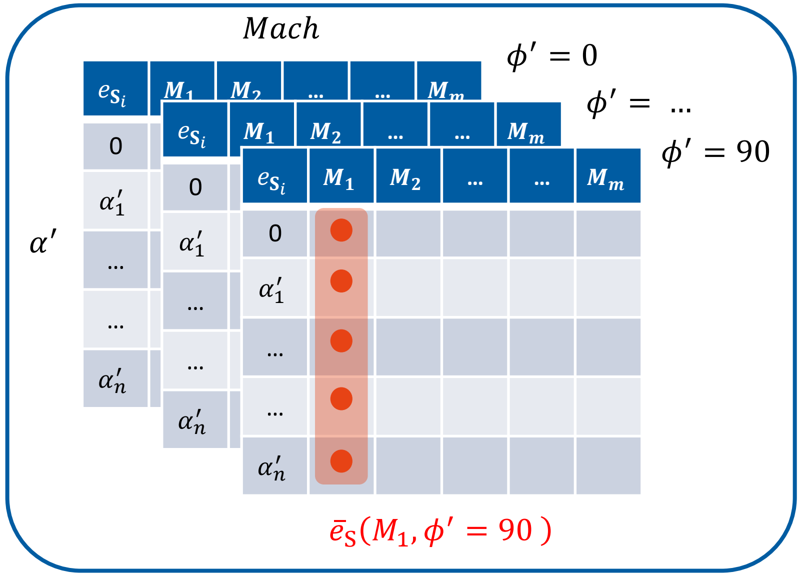

Figure 8. 3D table structure: example for the *Simple Linear Error* e_{S}.

Standard Deviation

$$\sigma_{\mathrm{S}}(M, \phi', \alpha') = \sqrt{\frac{\sum_{i=1}^{n}\left(e_{\mathrm{S}_i}(M, \phi', \alpha') - \bar{e}_{\mathrm{S}}(M, \phi', \alpha')\right)^2}{n}}$$

Normalized Mean Error

$$\bar{e}_{\mathrm{S_{Norm}}}(M, \phi', \alpha') = \frac{\bar{e}_{\mathrm{S}}(M, \phi', \alpha')}{\bar{C}_{\mathrm{CFD}}(M, \phi', \alpha')} \quad , \quad \begin{cases} \bar{e}_{\mathrm{S}}(M, \phi', \alpha') = \dfrac{\sum_{i=1}^{n}\left(C_{\mathrm{S}_i}(M, \phi', \alpha') - C_{\mathrm{CFD}_i}(M, \phi', \alpha')\right)}{n} \\ \bar{C}_{\mathrm{S}}(M, \phi', \alpha') = \dfrac{\sum_{i=1}^{n}\left(C_{\mathrm{S}_i}(M, \phi', \alpha')\right)}{n} \end{cases}$$

Model Comparison: Statistical Error Analysis

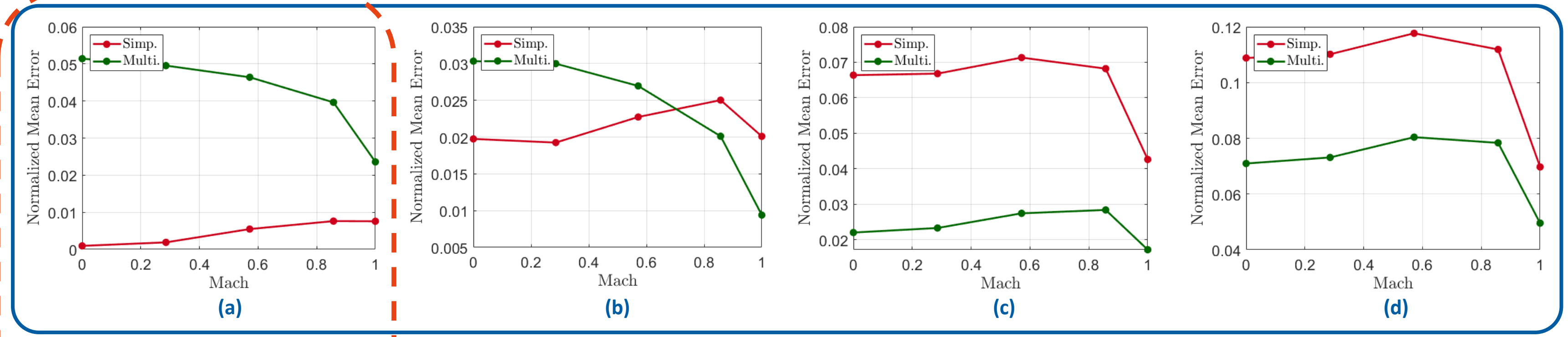

Figure 9. Normalized mean error related to the vertical force: (a) $\phi' = 0$ [deg], (b) (c) (d) for increasing values of ϕ'.

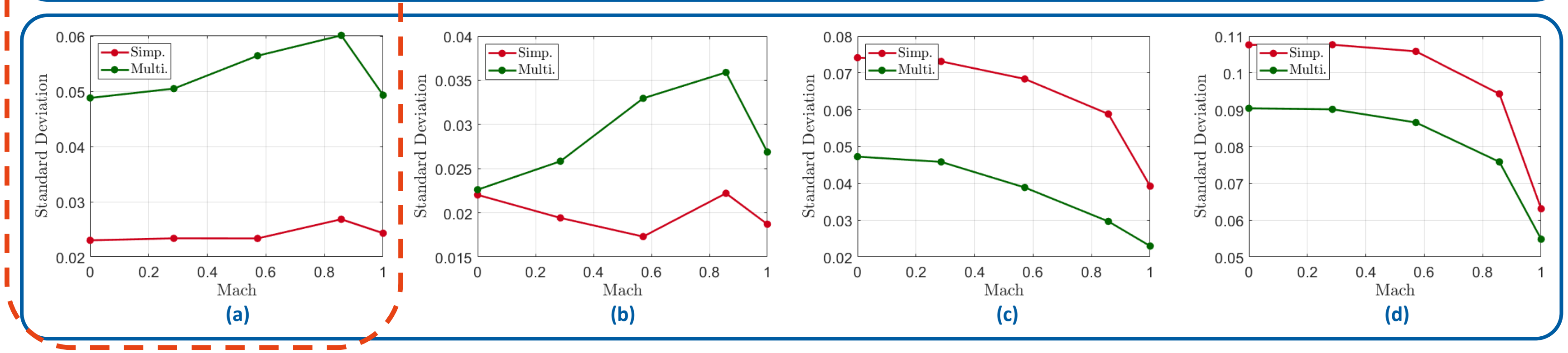

Figure 10. Standard deviation related to the vertical force: (a) $\phi' = 0$ [deg], (b) (c) (d) for increasing values of ϕ'.

For $\phi' = 0$ [deg], $\alpha' = \alpha$: the results show how the *Simple Linear Model* provides higher accuracy than the *Multivariable Model*.

By increasing the roll (ϕ'), and consequently, the impact of the sideslip angle (β) variation, the *Multivariable Model* shows better capability in modeling the aerodynamic behavior.

Model Comparison: Data Interpolation

- In the case of forces/moments highly dependents only on one of the angle variation (α or β), the interpolated surfaces generated by the different approaches provide similar results, as in Figure 11.
- However, in the case of high dependency on both the angle variations, the *Simple Linear Regression* shows its limited accuracy, as in Figures 12 and 13.

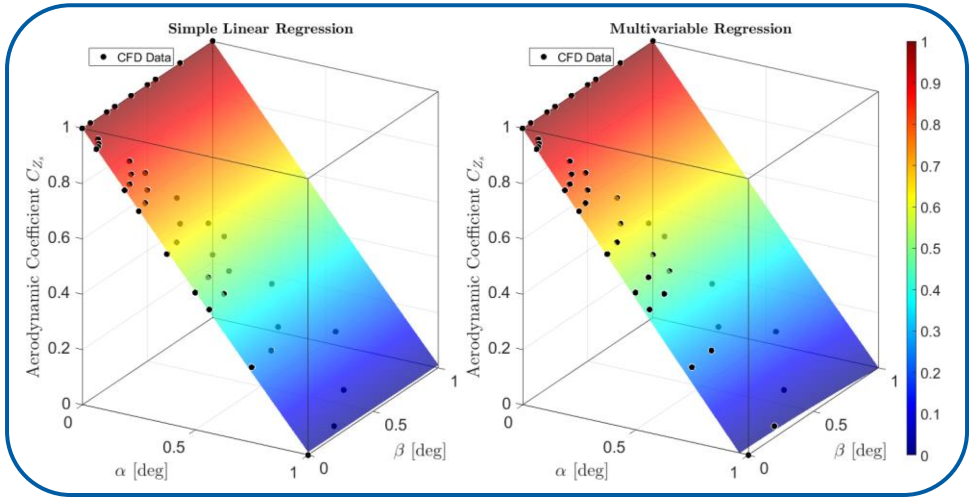

Figure 11. Interpolated surfaces comparison: vertical force.

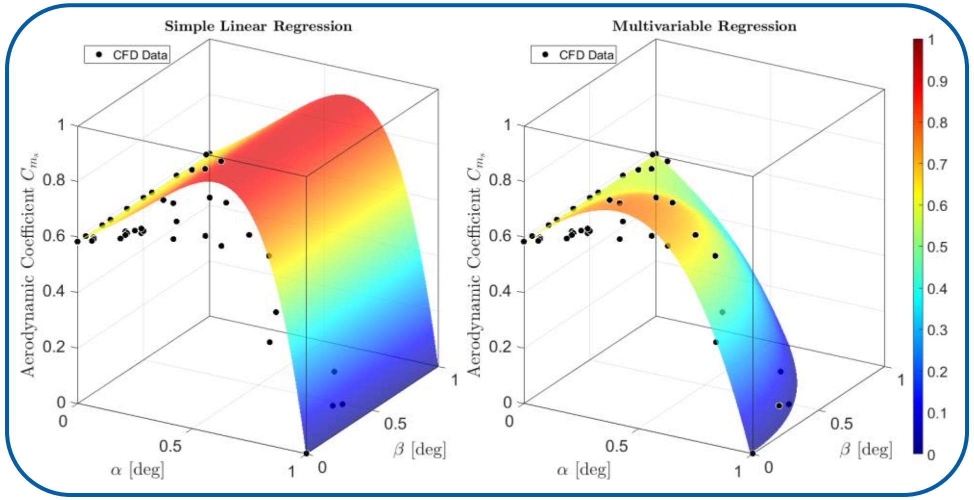

Figure 12. Interpolated surfaces comparison: pitching moment.

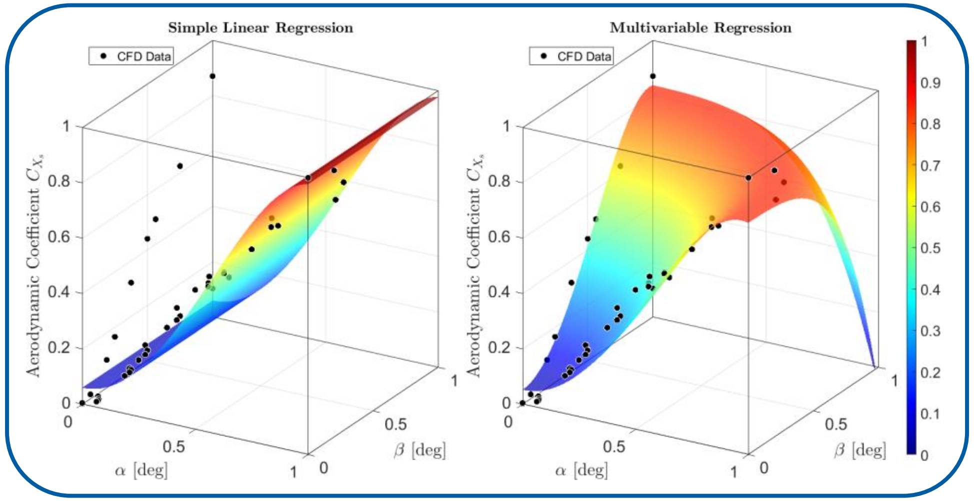

Figure 13. Interpolated surfaces comparison: longitudinal force.

NB: All the presented data have been rescaled for confidentiality reasons.

Conclusions

- CFD static characterization of the new LRGP concept.
- Investigation of different regression approaches (Simple Linear Regression, Multivariable Regression).
- Accuracy assessment of several regression functions for each of the aerodynamic coefficients.
- Statistical analysis on the interpolation errors and cross comparison between the model performances.
- Graphical verification of the data fitting capability of the interpolated surfaces.

Identification of the most reliable regression model for each of the investigated approaches.

Final accuracy comparison between the regression approaches.

Higher reliability provided by the Multivariable Regression approach.

Thank you for your kind attention.

Any questions ?

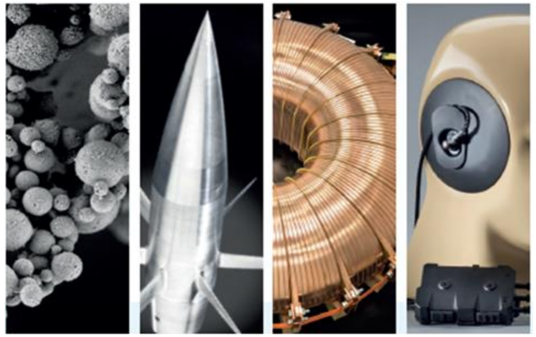

ISL - French-German Research Institute of Saint-Louis
University Grenoble Alpes, Grenoble INP, GIPSA-lab

Gian Marco VINCO
Gian-Marco.Vinco@isl.eu

Appendix

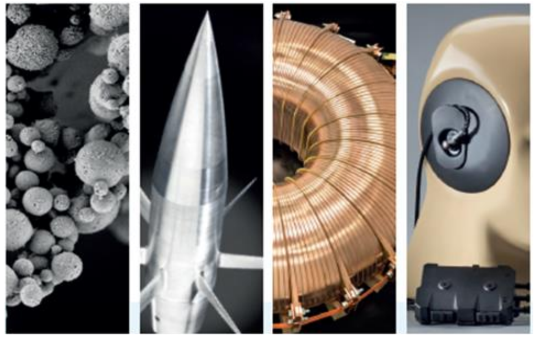

ISL - French-German Research Institute of Saint-Louis
University Grenoble Alpes, Grenoble INP, GIPSA-lab

Gian Marco VINCO
Gian-Marco.Vinco@isl.eu

Cartesian Coordinates

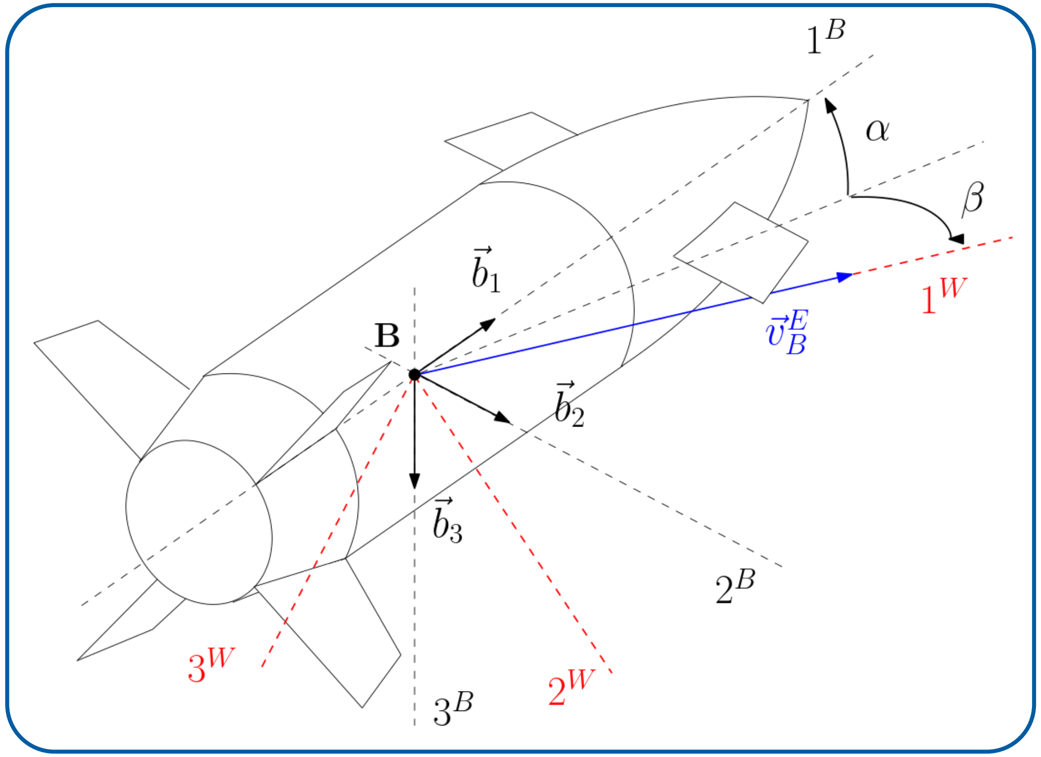

Polar Coordinates

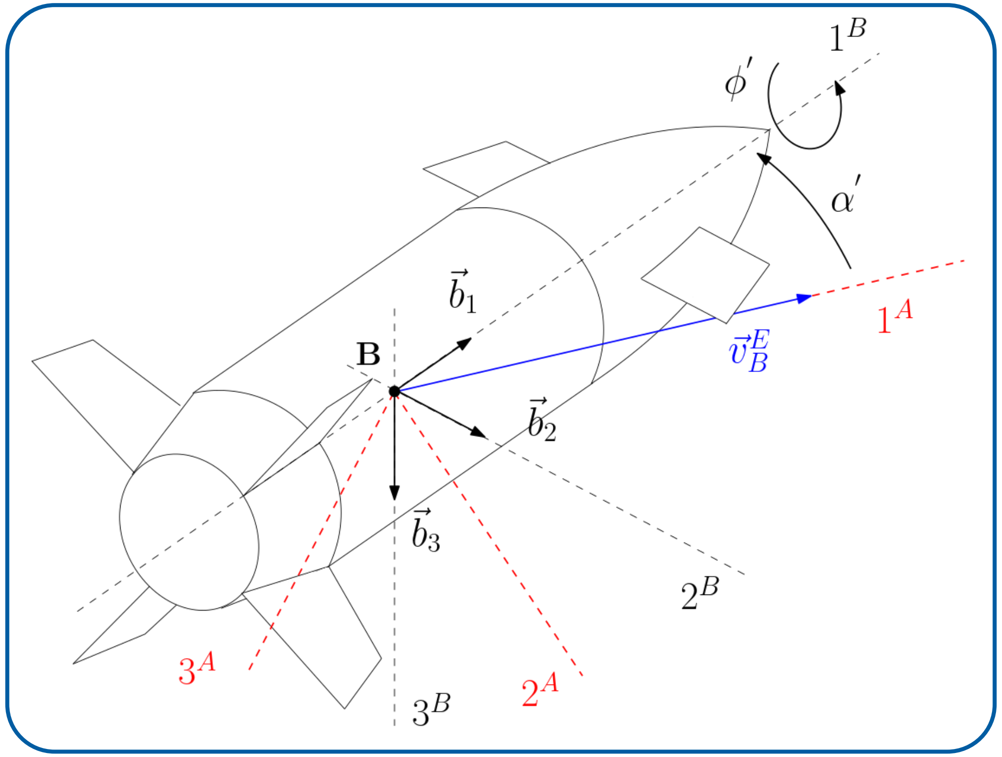

- Frame base vectors.
  - Body (B): $\vec{b}_1, \vec{b}_2, \vec{b}_3$.
- Coordinate axes.
  - Body (B): $1^B, 2^B, 3^B$.
  - Wind (W): $1^W, 2^W, 3^W$.

- Frame base vectors.
  - Body (B): $\vec{b}_1, \vec{b}_2, \vec{b}_3$.
- Coordinate axes.
  - Body (B): $1^B, 2^B, 3^B$.
  - Wind (A): $1^A, 2^A, 3^A$.

Appendix : α Derivatives Analysis

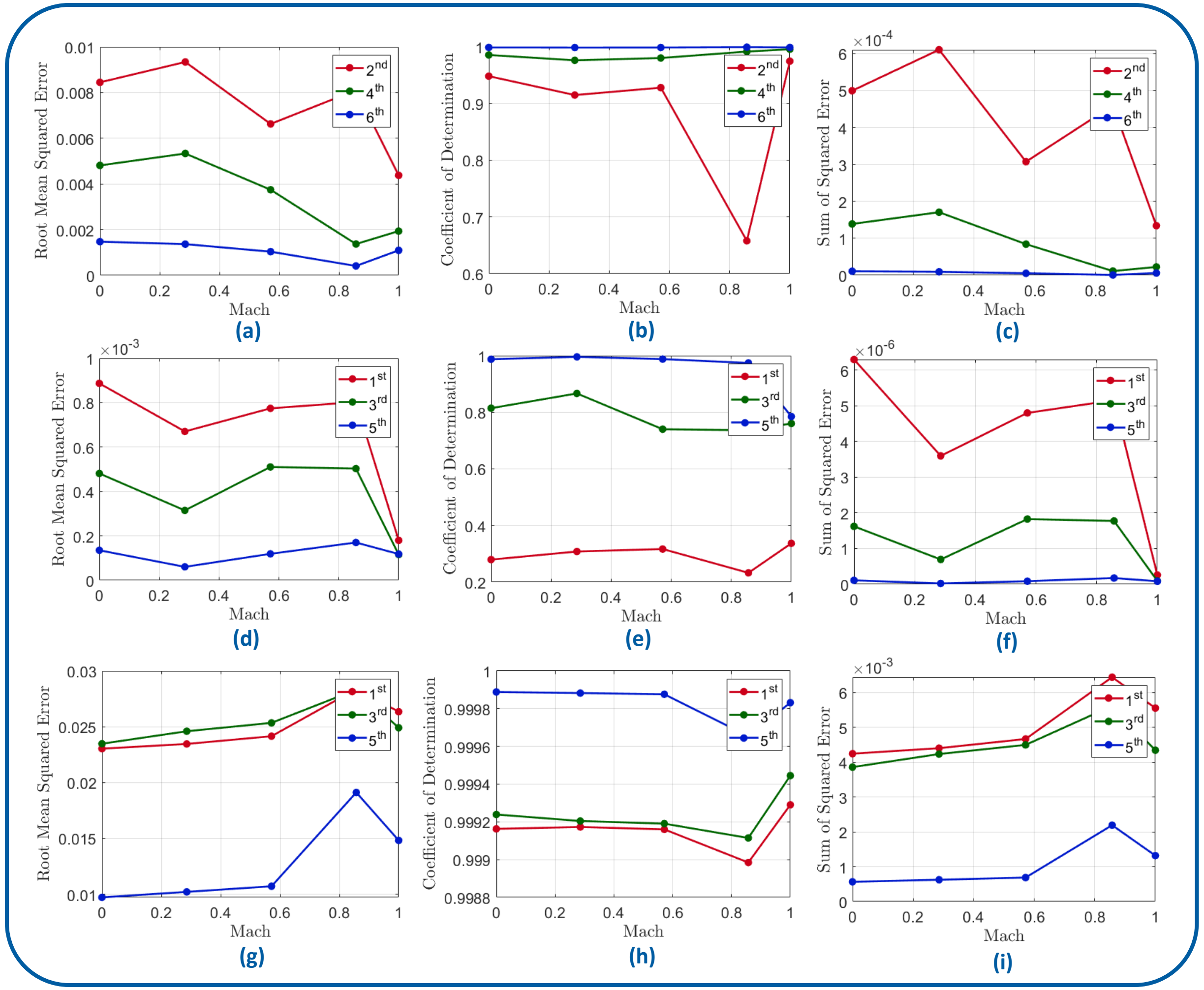

Figure 1. Regression accuracy results for the α coefficient derivatives : RMSE, R^2, and SSE, respectively for the longitudinal ((a),(b),(c)), the lateral ((d),(e),(f)) and the vertical ((g),(h),(i)) forces.

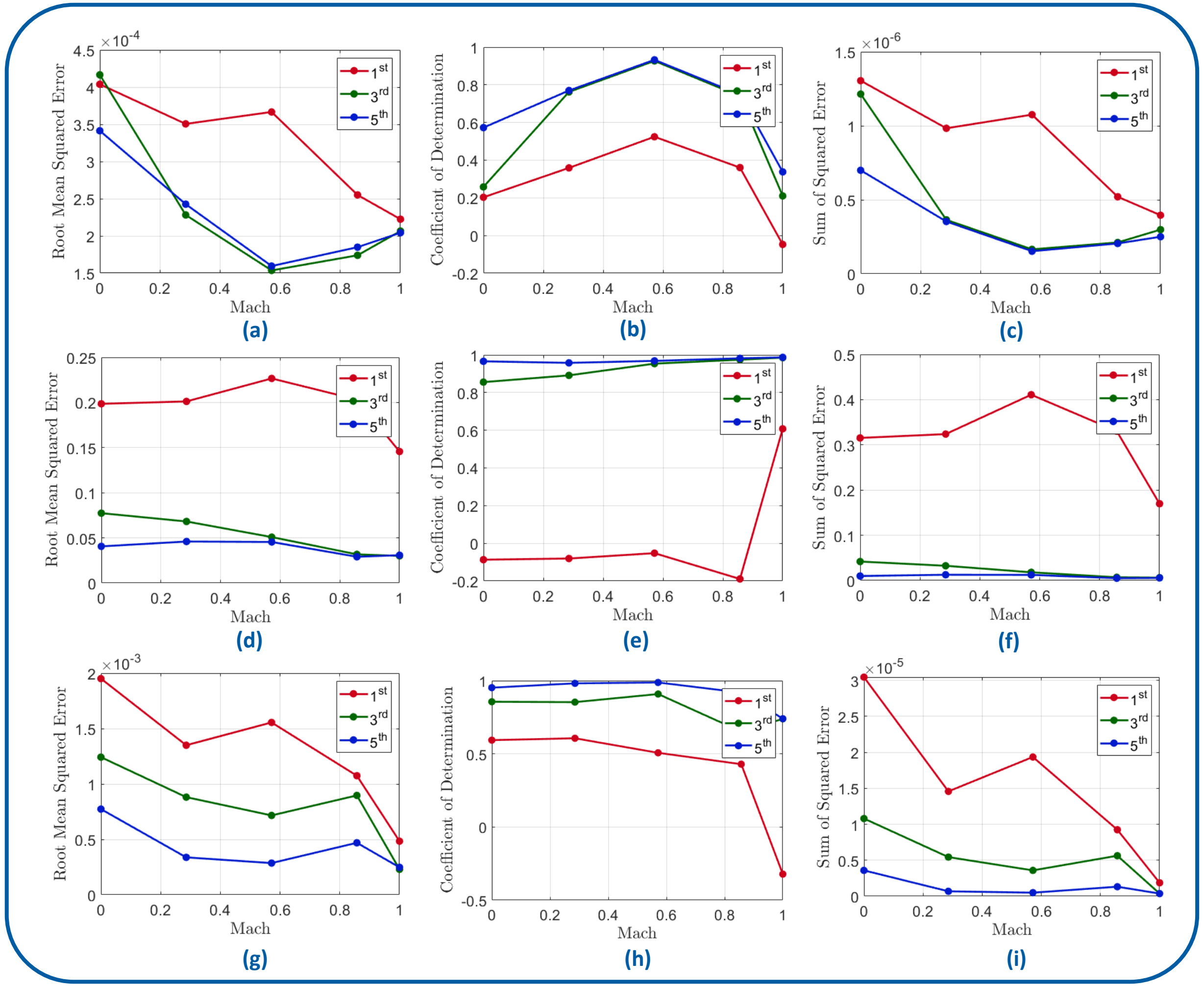

Figure 2. Regression accuracy results for the α coefficient derivatives : RMSE, R^2, and SSE, respectively for the roll ((a),(b),(c)), the pitch ((d),(e),(f)) and the yaw ((g),(h),(i)) moments.

Appendix : α Interpolation Results

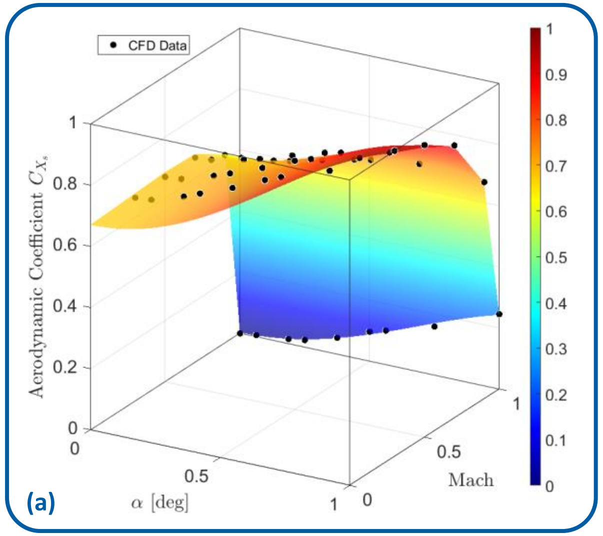

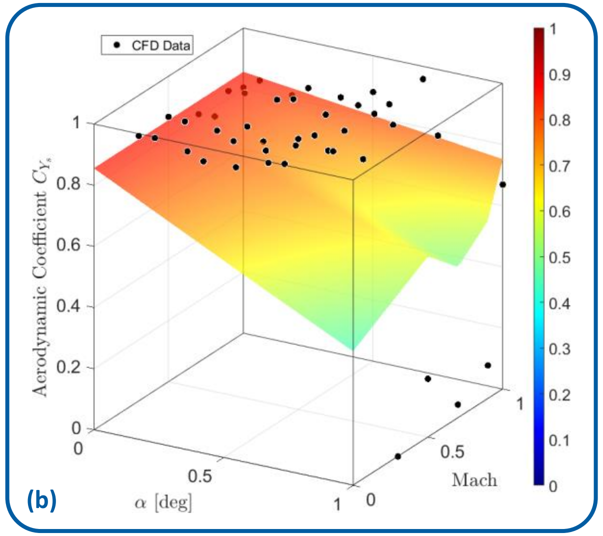

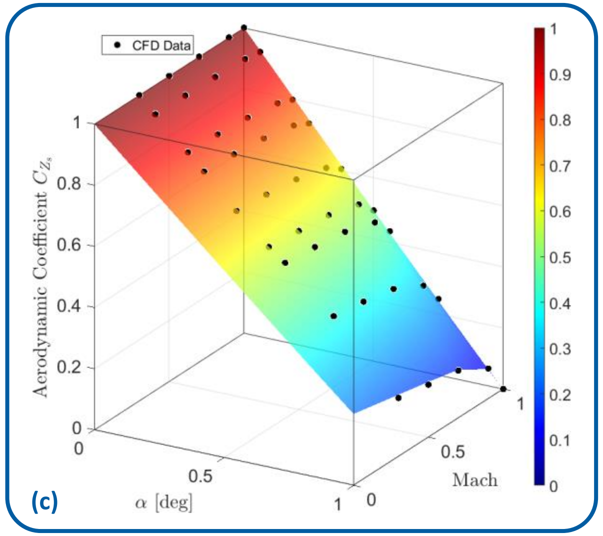

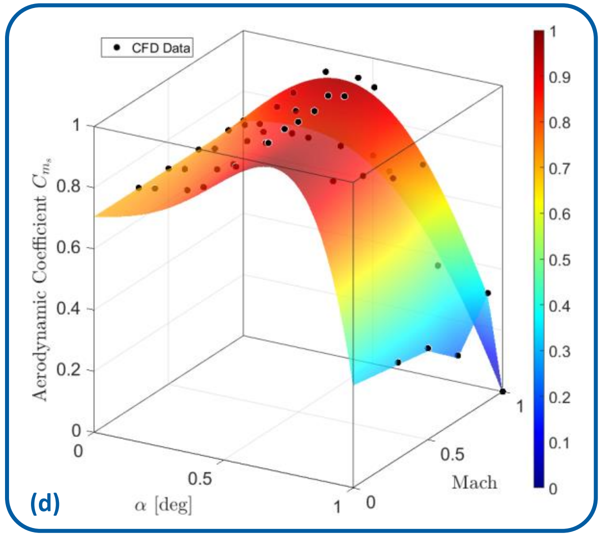

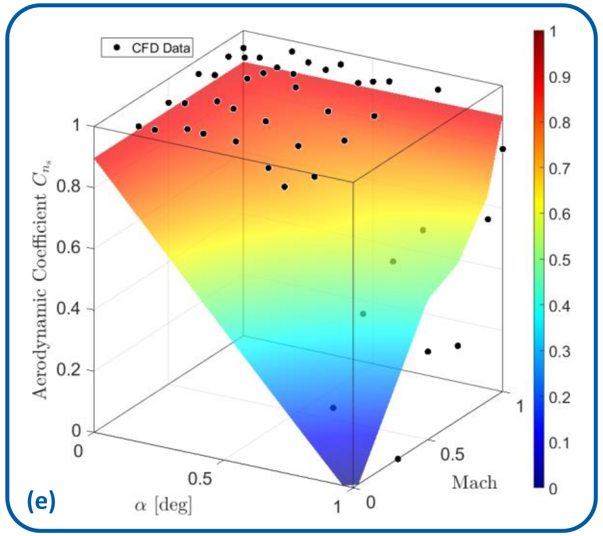

Figure 3. Interpolations results of the α coefficient derivatives:

- (a) longitudinal force,
- (b) lateral force,
- (c) vertical force,
- (d) pitch moment,
- (e) yaw moment.

ISL

Appendix : β Derivatives Analysis

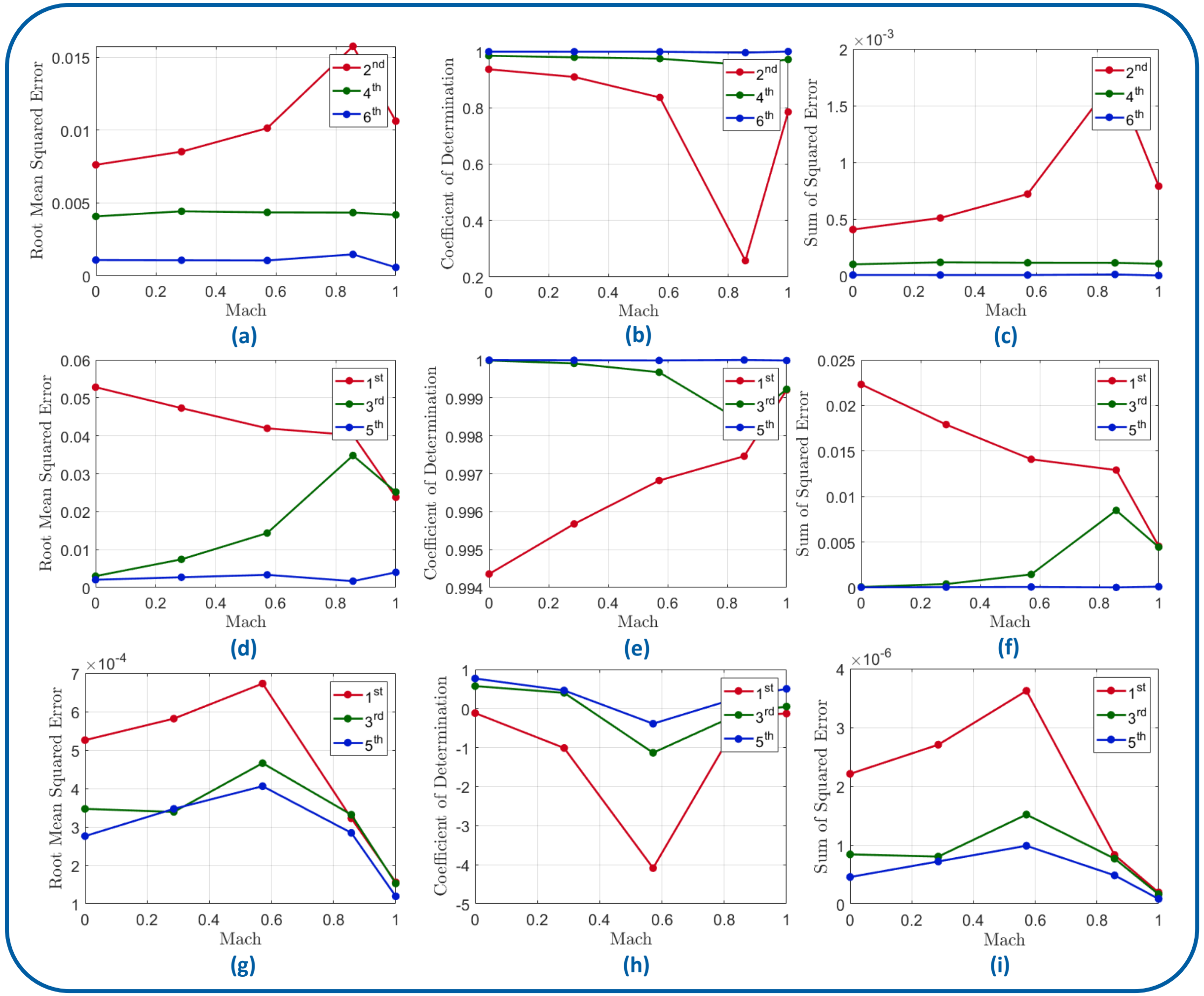

Figure 4. Regression accuracy results for the β coefficient derivatives : RMSE, R^2, and SSE, respectively for the longitudinal ((a),(b),(c)), the lateral ((d),(e),(f)) and the vertical ((g),(h),(i)) forces.

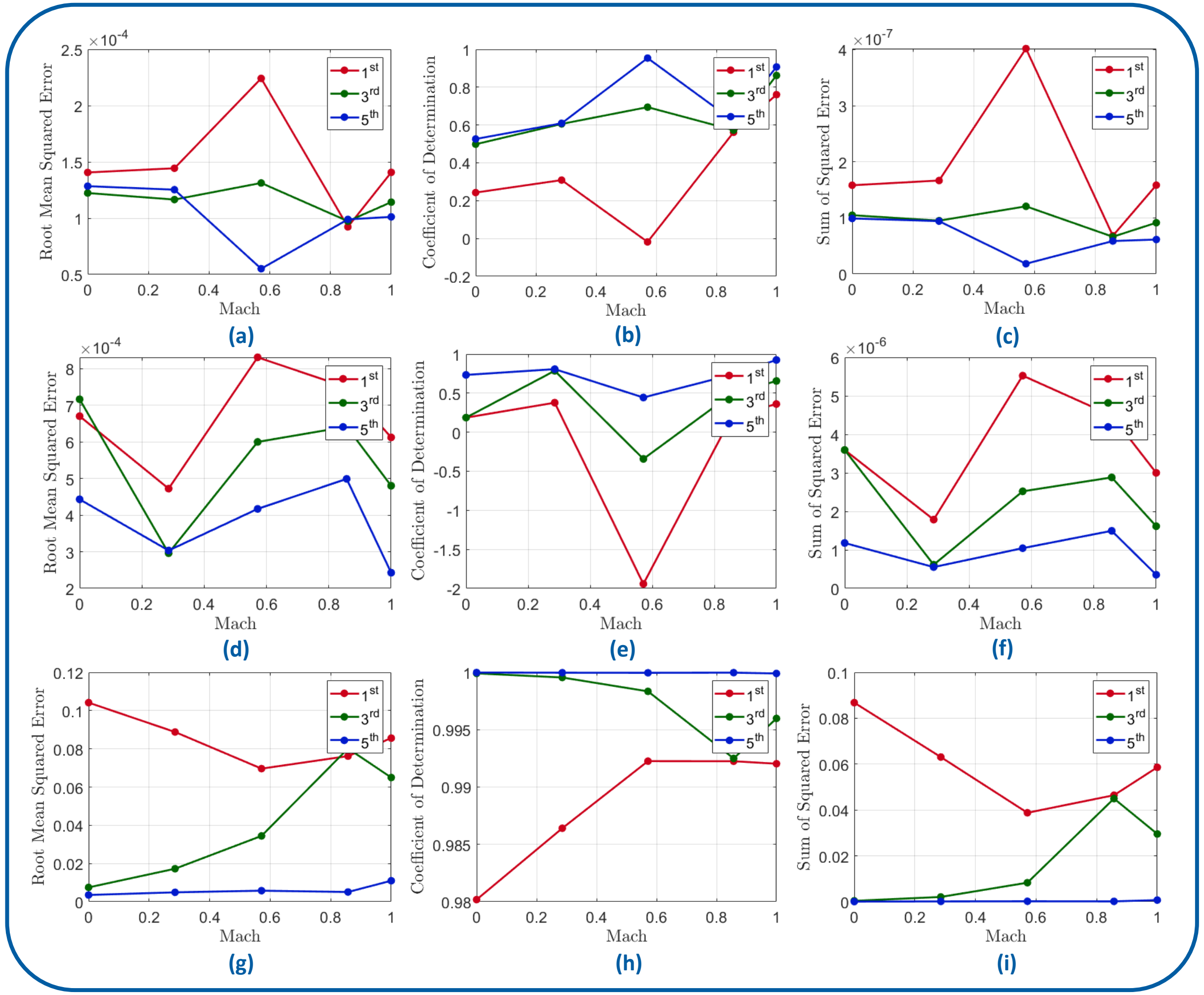

Figure 5. Regression accuracy results for the β coefficient derivatives : RMSE, R^2, and SSE, respectively for the roll ((a),(b),(c)), the pitch ((d),(e),(f)) and the yaw ((g),(h),(i)) moments.

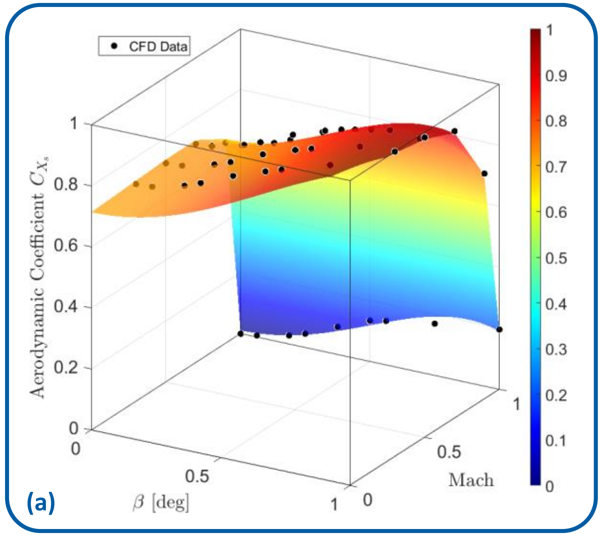

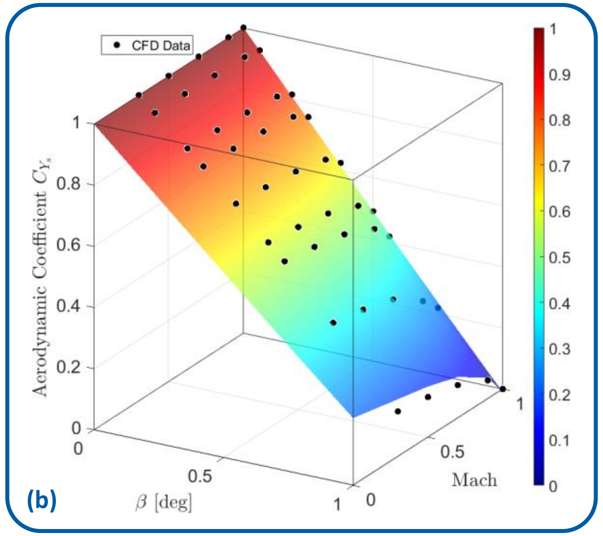

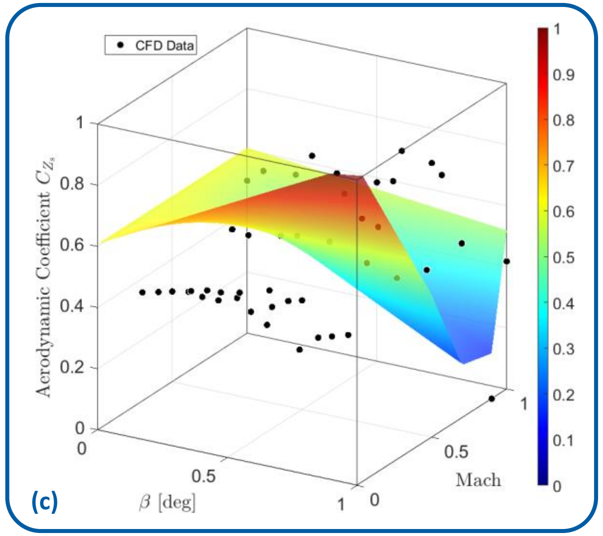

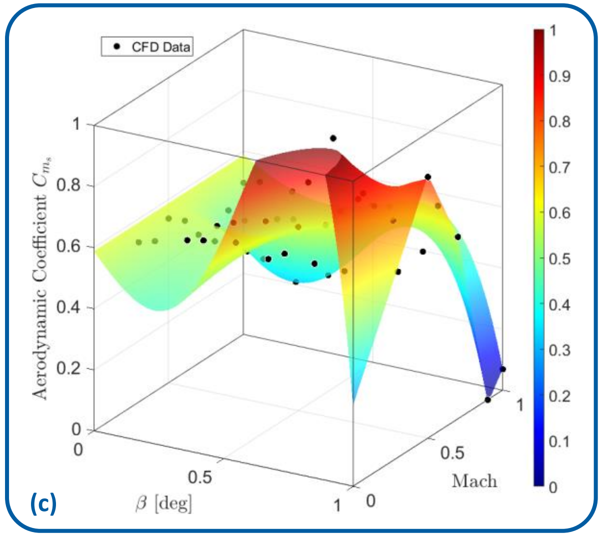

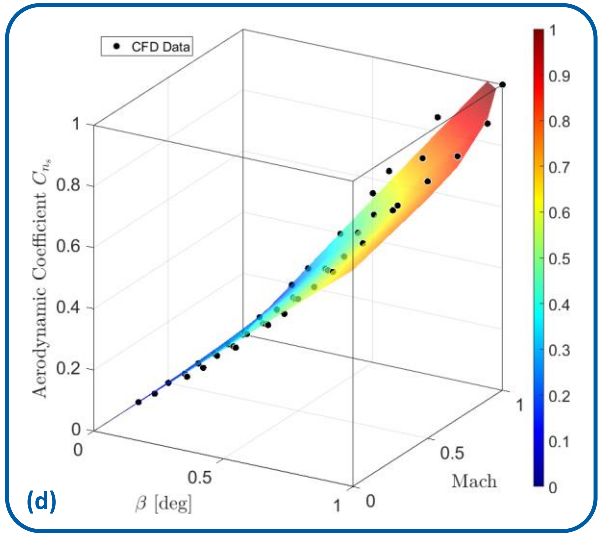

Figure 6. Interpolations results of the β coefficient derivatives:

- (a) longitudinal force,
- (b) lateral force,
- (c) vertical force,
- (d) pitch moment,
- (e) yaw moment.

Flight Mechanics EoM: Aerodynamic Forces [1] [2]

$$[f_B^P]^B = \bar{q}S \begin{bmatrix} -(C_D \cos\alpha \cos\beta - C_{L_\alpha}(1-\cos^2\alpha \cos^2\beta)) \\ -(C_D + C_{L_\alpha} \cos\alpha \cos\beta)\sin\beta \\ -(C_D + C_{L_\alpha} \cos\alpha \cos\beta) \cos\beta \sin\alpha \end{bmatrix} = \bar{q}S \begin{bmatrix} -C_{A_S} \\ -C_{N_\alpha}\sin\beta \\ -C_{N_\alpha} \cos\beta \sin\alpha \end{bmatrix} = \bar{q}S \begin{bmatrix} -C_{A_S} \\ +C_{Y_S} \\ -C_{N_S} \end{bmatrix} = \bar{q}S \begin{bmatrix} +C_{X_S} \\ +C_{Y_S} \\ +C_{Z_S} \end{bmatrix}$$

Multivariable Regression Model

$$C_{X_s}(M,\alpha,\beta) = C_{X_0}(M) + C_{X_2}(M)\cos\alpha\cos\beta + C_{X_4}(M)\cos^2\alpha\cos^2\beta$$

$$C_{Y_s}(M,\alpha,\beta) = C_{Y_2}(M)\sin\beta\cos\alpha$$

$$C_{Z_s}(M,\alpha,\beta) = C_{Z_2}(M)\sin\alpha\cos\beta$$

[1] McCoy, R. (1999). *Modern exterior ballistics: the launch and flight dynamics of symmetric projectiles,* Schiffer.
[2] Zipfel, P. (2014). *Modeling and simulation of aerospace vehicle dynamics*. American Institute of Aeronautics and Astronautics.

$$C_\mathrm{X}\begin{cases}\mathbf{T:}\quad C_\mathrm{X}(M,\alpha,\beta)=C_{\mathrm{X}_0}(M)+C_{\mathrm{X}_2}(M)(\sin^2\alpha+\sin^2\beta)+C_{\mathrm{X}_4}(M)(\sin^4\alpha+\sin^4\beta)\\ \mathbf{F:}\quad C_\mathrm{X}(M,\alpha,\beta)=C_{\mathrm{X}_0}(M)+C_{\mathrm{X}_2}(M)\cos\alpha\cos\beta+C_{\mathrm{X}_4}(M)\cos^2\alpha\cos^2\beta\\ \mathbf{I:}\quad C_\mathrm{X}(M,\alpha,\beta)=C_{\mathrm{X}_0}(M)+C_{\mathrm{X}_{\alpha 2}}(M)\sin^2\alpha+C_{\mathrm{X}_{\beta 2}}(M)\sin^2\beta+C_{\mathrm{X}_{\alpha 4}}(M)\sin^4\alpha+C_{\mathrm{X}_{\beta 4}}(M)\sin^4\beta\end{cases}$$

$$C_\mathrm{Y}\begin{cases}\mathbf{T:}\quad C_\mathrm{Y}(M,\alpha,\beta)=C_{\mathrm{Y}_1}(M)\sin\beta\cos\alpha+C_{\mathrm{Y}_3}(M)\sin^3\beta\cos\alpha\\ \mathbf{F:}\quad C_\mathrm{Y}(M,\alpha,\beta)=C_{\mathrm{Y}_\beta}(M)\sin\beta\cos\alpha\\ \mathbf{I:}\quad C_\mathrm{Y}(M,\alpha,\beta)=C_{\mathrm{Y}_{\beta 1}}(M)\sin\beta+C_{\mathrm{Y}_{\alpha 1}}(M)\sin\alpha\end{cases}$$

$$C_\mathrm{Z}\begin{cases}\mathbf{T:}\quad C_\mathrm{Z}(M,\alpha,\beta)=C_{\mathrm{Z}_1}(M)\sin\alpha\cos\beta+C_{\mathrm{Z}_3}(M)\sin^3\alpha\cos\beta\\ \mathbf{F:}\quad C_\mathrm{Z}(M,\alpha,\beta)=C_{\mathrm{Z}_1}(M)\sin\alpha\cos\beta\\ \mathbf{I:}\quad C_\mathrm{Z}(M,\alpha,\beta)=C_{\mathrm{Z}_{\alpha 1}}(M)\sin\alpha+C_{\mathrm{Z}_{\beta 1}}(M)\sin\beta\end{cases}$$

$$C_\mathrm{m}\begin{cases}\mathbf{T:}\quad C_\mathrm{m}(M,\alpha,\beta)=C_{\mathrm{m}_1}(M)\sin\alpha\cos\beta+C_{\mathrm{m}_3}(M)\sin^3\alpha\cos\beta\\ \mathbf{F:}\quad C_\mathrm{m}(M,\alpha,\beta)=C_{\mathrm{m}_1}(M)\sin\alpha\cos\beta+C_{\mathrm{m}_3}(M)\sin\alpha\cos\alpha\cos^2\beta\\ \mathbf{I:}\quad C_\mathrm{m}(M,\alpha,\beta)=C_{\mathrm{m}_{\alpha 1}}(M)\sin\alpha+C_{\mathrm{m}_{\beta 1}}(M)\sin\beta+C_{\mathrm{m}_{\alpha 3}}(M)\sin^3\alpha+C_{\mathrm{m}_{\beta 3}}(M)\sin^3\beta\end{cases}$$

T : Test
F : Formula
I : Independent

Appendix : α & β Derivatives Analysis

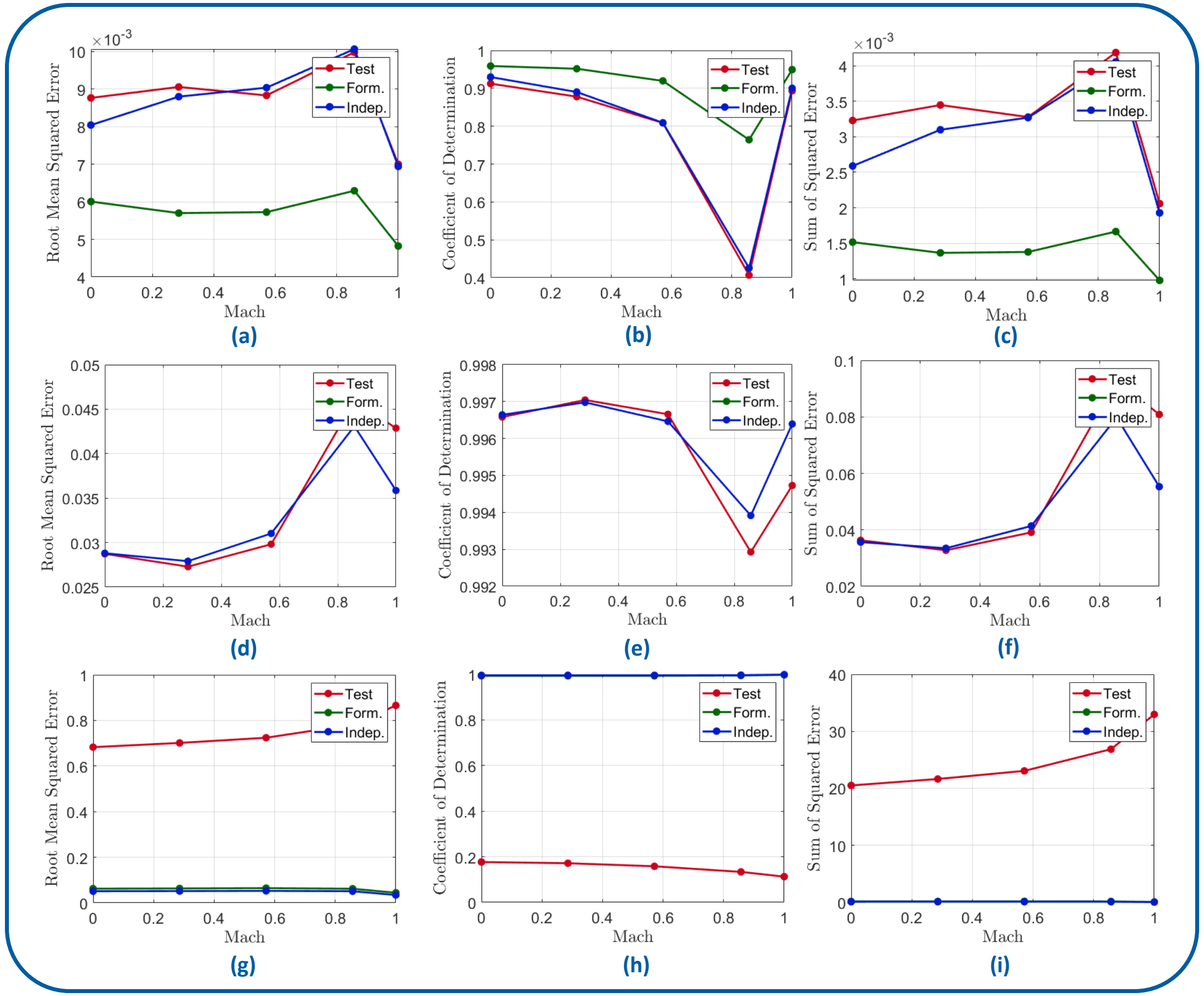

Figure 7. Regression accuracy results for the α & β coefficient derivatives : RMSE, R^2, and SSE, respectively for the longitudinal ((a),(b),(c)), the lateral ((d),(e),(f)) and the vertical ((g),(h),(i)) forces.

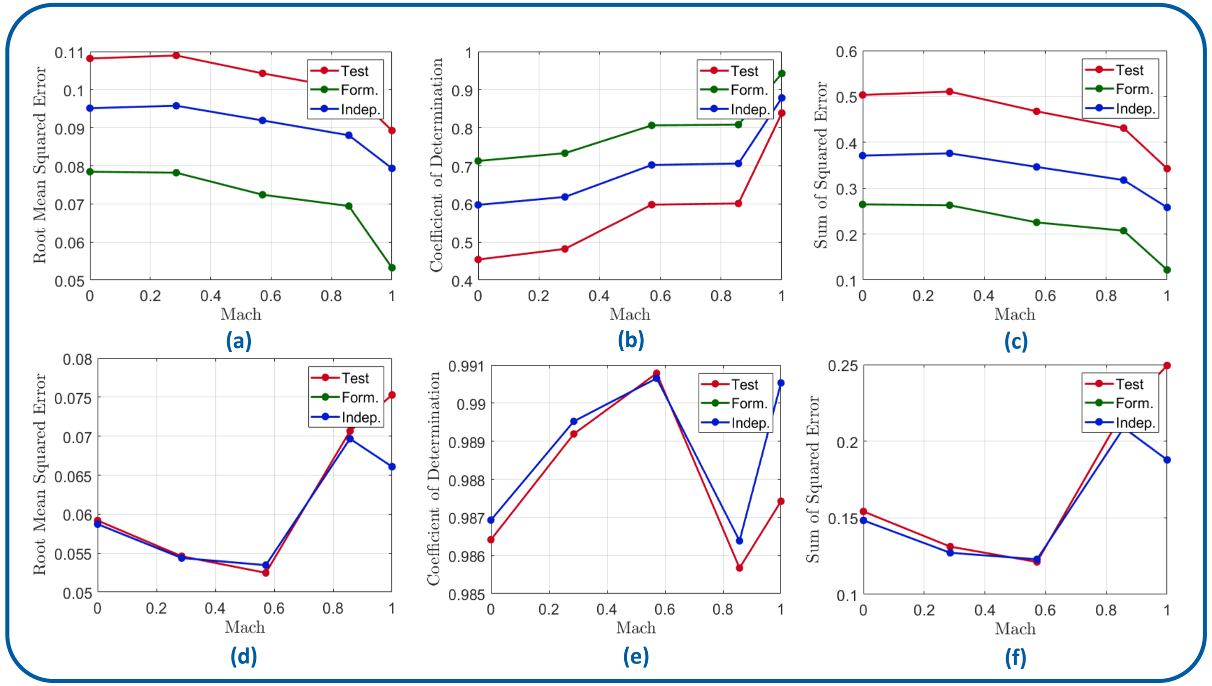

Figure 5. Regression accuracy results for the α & β coefficient derivatives : RMSE, R^2, and SSE, respectively for the pitch ((a),(b),(c)) and the yaw ((d),(e),(f)) moments.

Appendix : α & β Interpolation Results

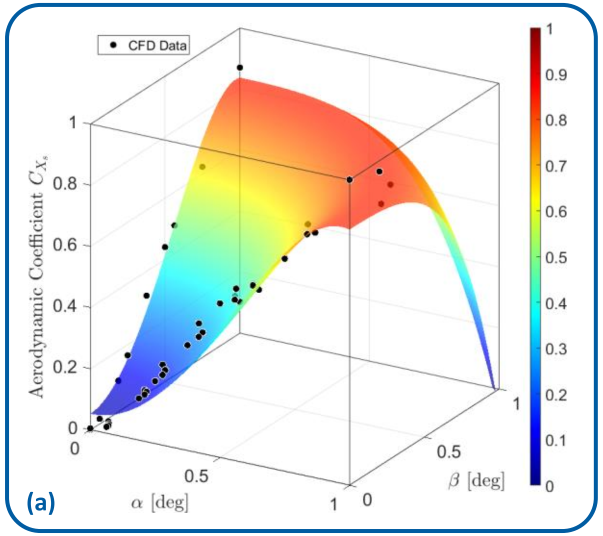

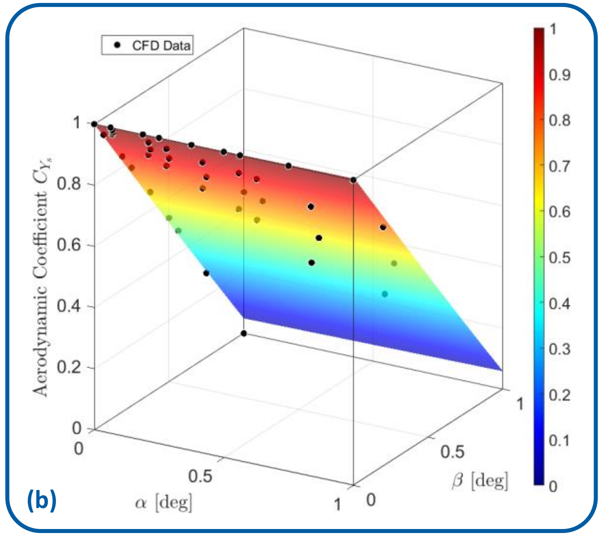

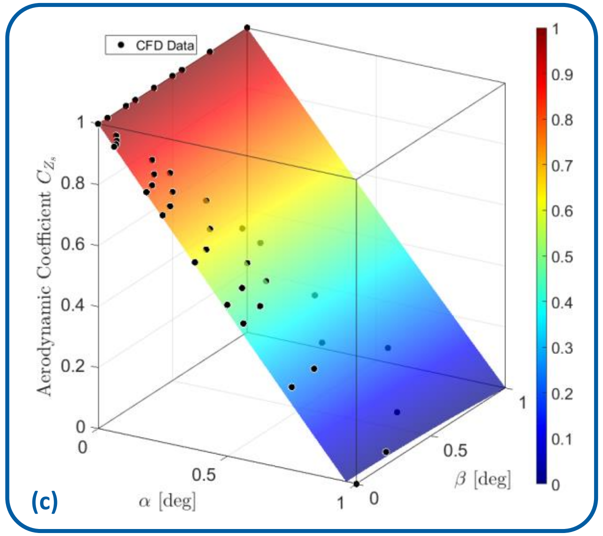

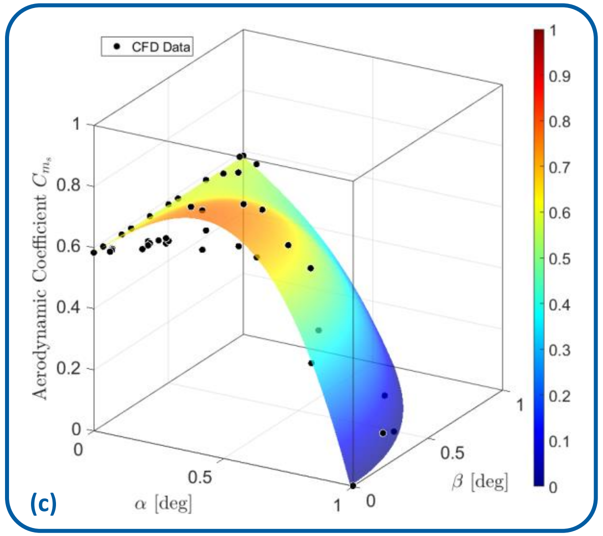

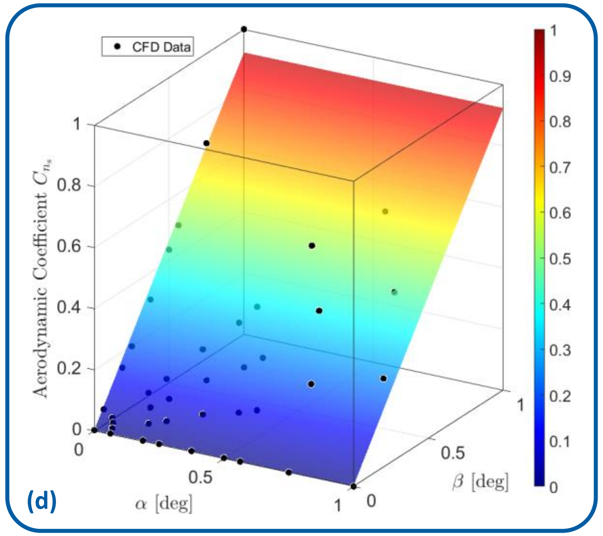

Figure 9. Interpolations results of the α & β coefficient derivatives:

- (a) longitudinal force,
- (b) lateral force,
- (c) vertical force,
- (d) pitch moment,
- (e) yaw moment.

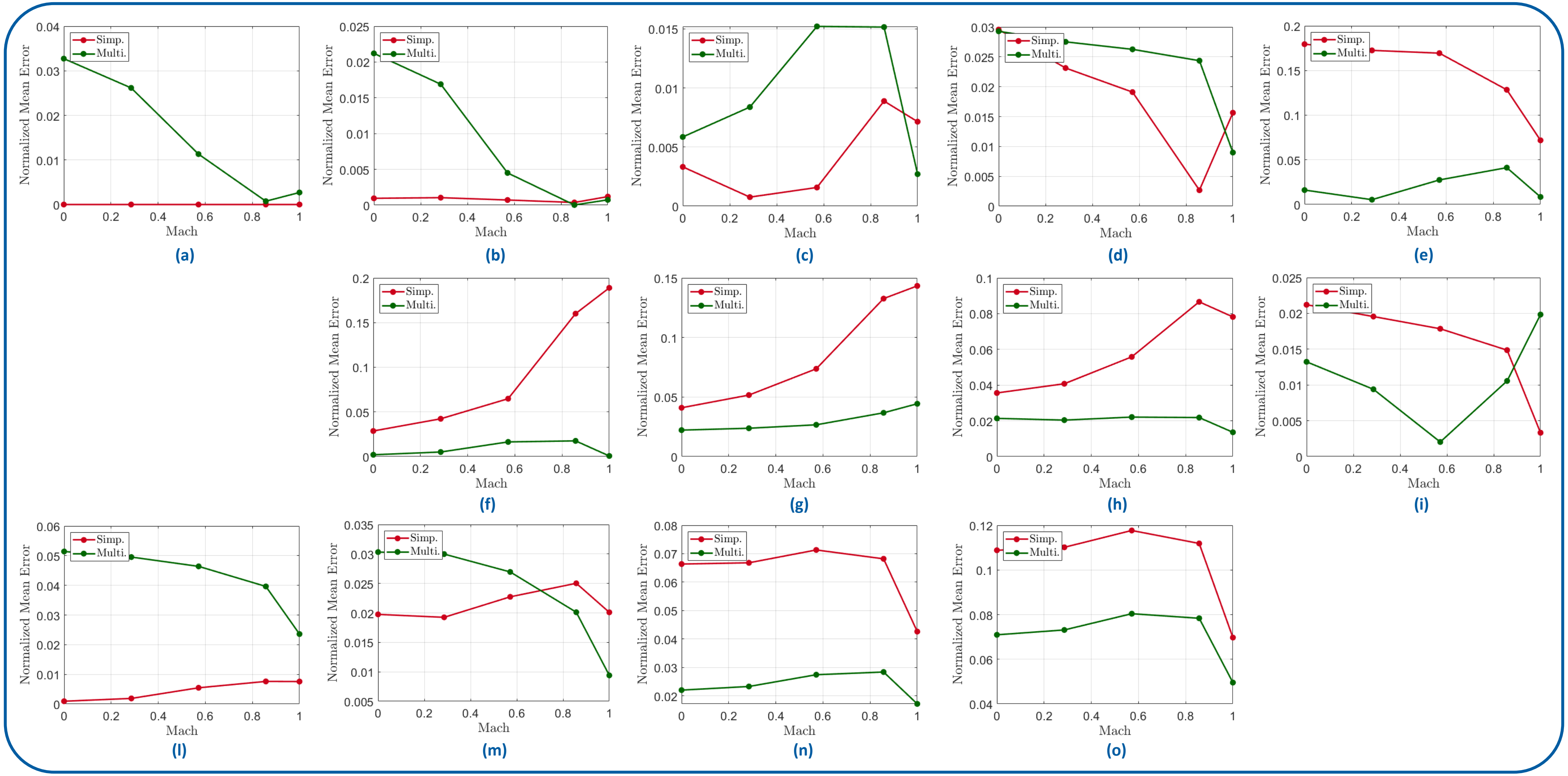

Figure 10. Models comparison results: *Normalized Mean Error* for increasing values of the roll angle ϕ', starting from $\phi' = 0$ [deg] for the (a) and (l) plot column, up to $\phi' = 90$ [deg] for the (e) and (i) plot column. In particular, the graphs show the comparison results for the longitudinal (a)(b)(c)(d)(e), the lateral (f)(g)(h)(i) and the vertical (l)(m)(n)(o) forces.

Appendix : Normalized Mean Error Results

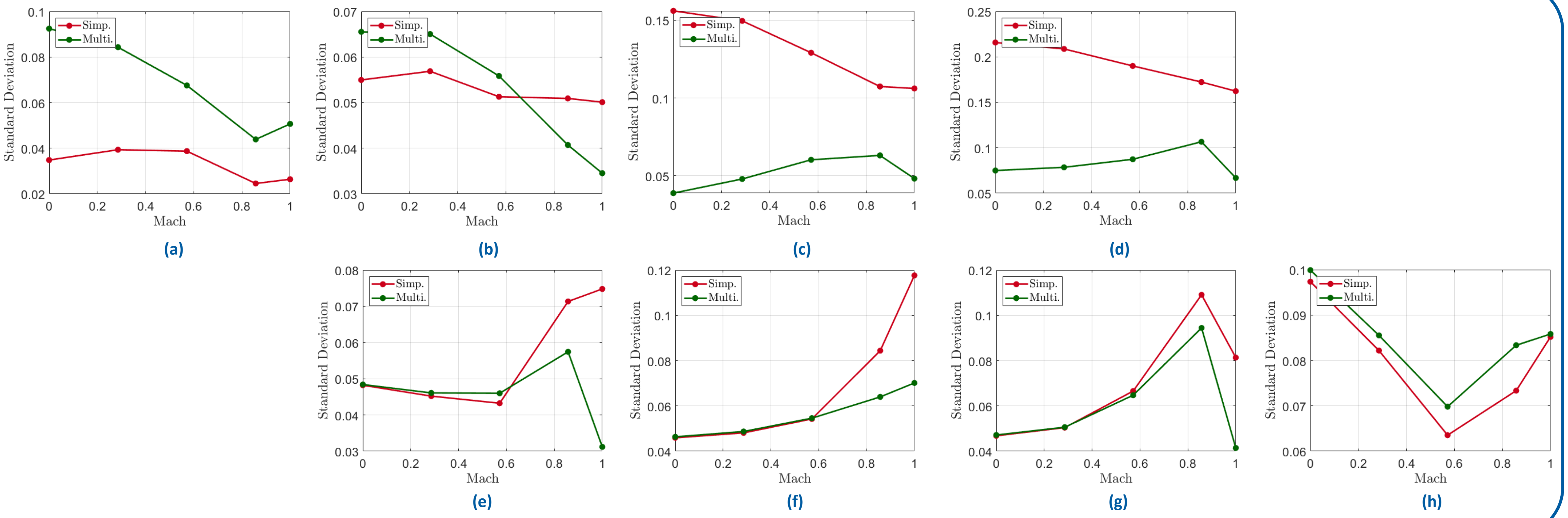

Figure 11. Models comparison results: *Normalized Mean Error* for increasing values of the roll angle ϕ', starting from $\phi' = 0$ [deg] for the (a) and (l) plot column, up to $\phi' = 90$ [deg] for the (e) and (i) plot column. In particular, the graphs show the comparison results for the pitch (a)(b)(c)(d) and the yaw (e)(f)(g)(h) moments.

Appendix : Standard Deviation Results

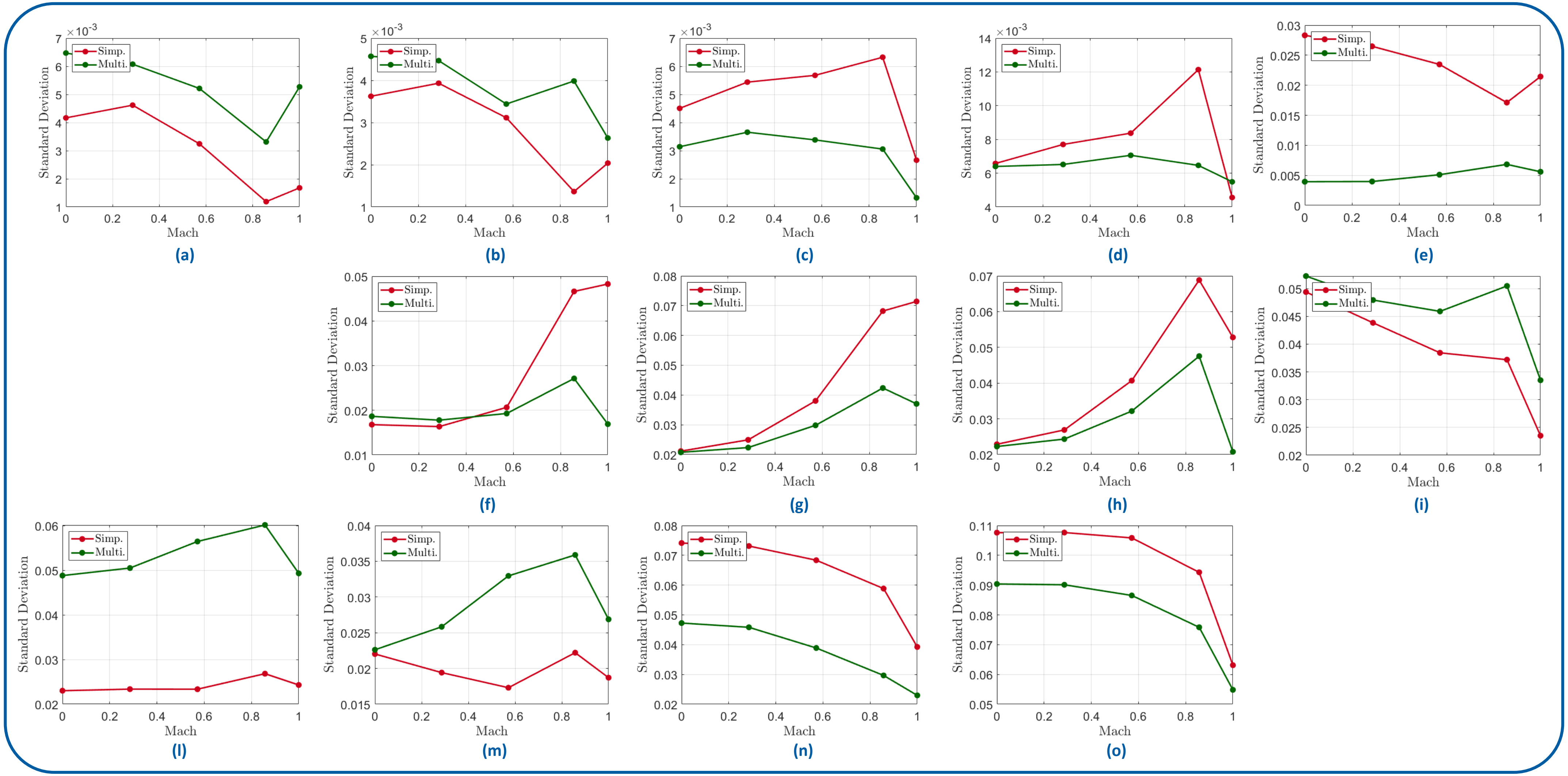

Figure 12. Models comparison results: *Standard Deviation* for increasing values of the roll angle ϕ', starting from $\phi' = 0$ [deg] for the (a) and (l) plot column, up to $\phi' = 90$ [deg] for the (e) and (i) plot column. In particular, the graphs show the comparison results for the longitudinal (a)(b)(c)(d)(e), the lateral (f)(g)(h)(i) and the vertical (l)(m)(n)(o) forces.

Appendix : Standard Deviation Results

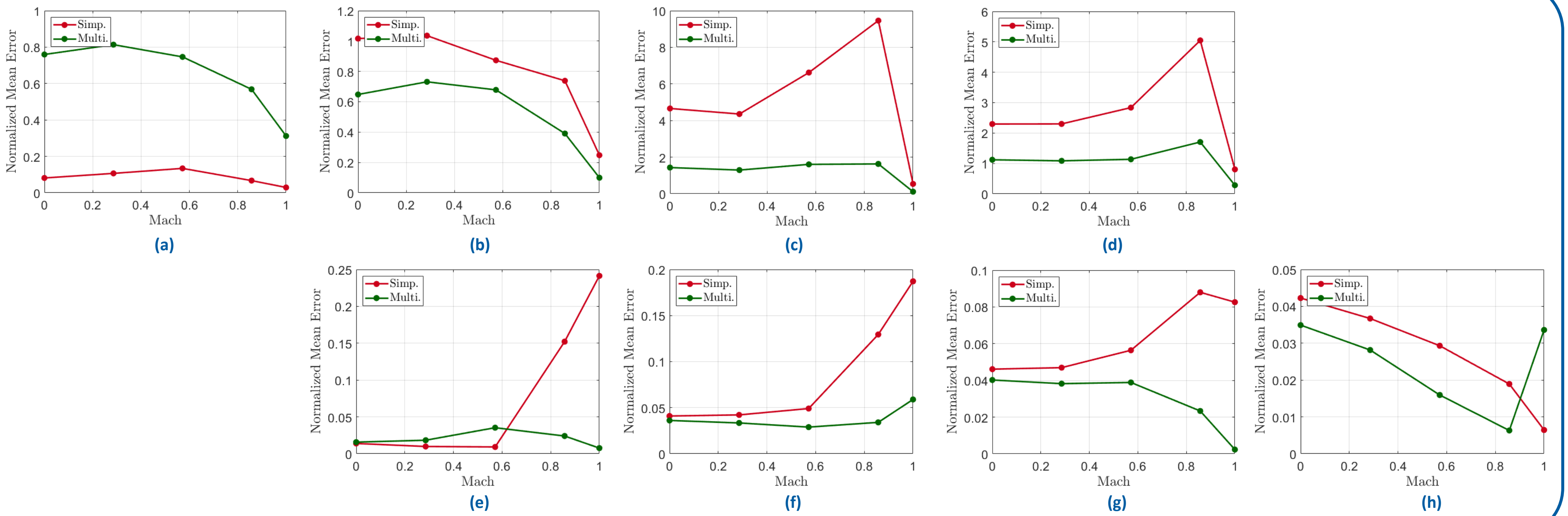

Figure 13. Models comparison results: *Standard Deviation* for increasing values of the roll angle ϕ', starting from $\phi' = 0$ [deg] for the (a) and (l) plot column, up to $\phi' = 90$ [deg] for the (e) and (i) plot column. In particular, the graphs show the comparison results for the pitch (a)(b)(c)(d) and the yaw (e)(f)(g)(h) moments.

Appendix : Models Interpolation Comparison

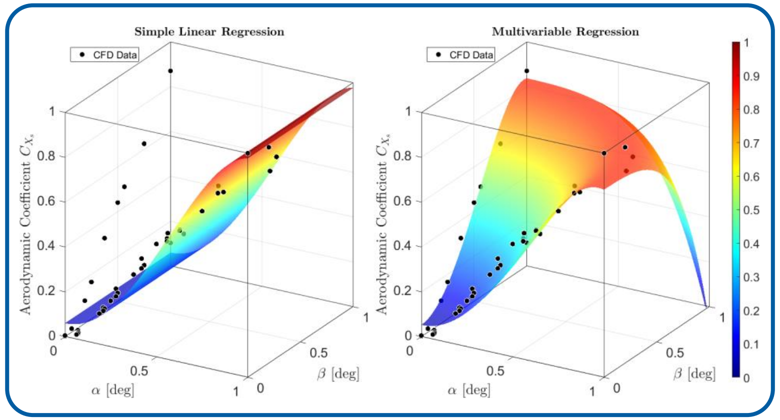

(a)

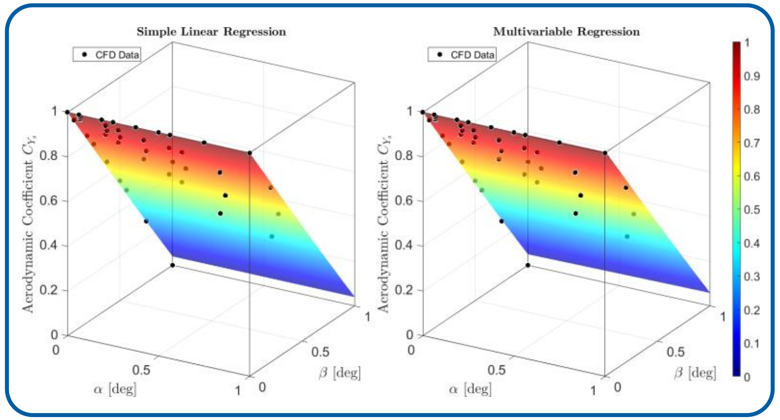

(b)

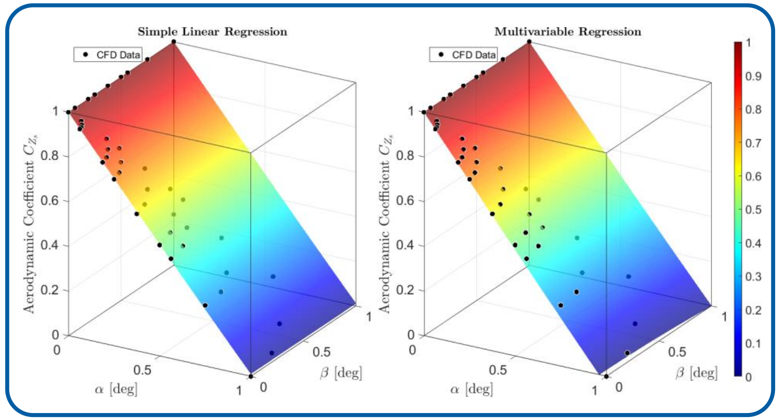

(c)

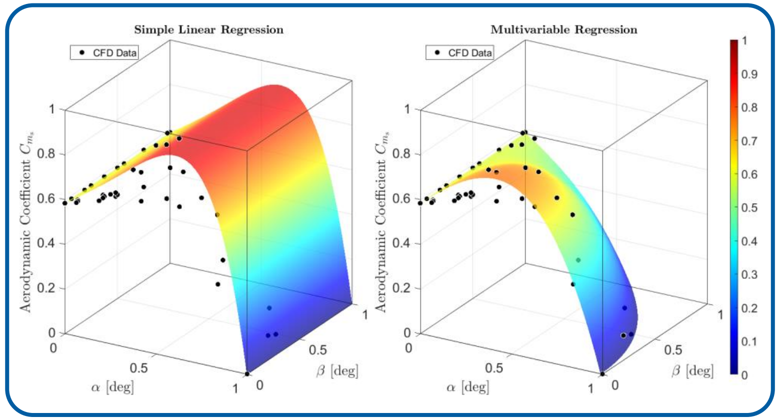

(d)

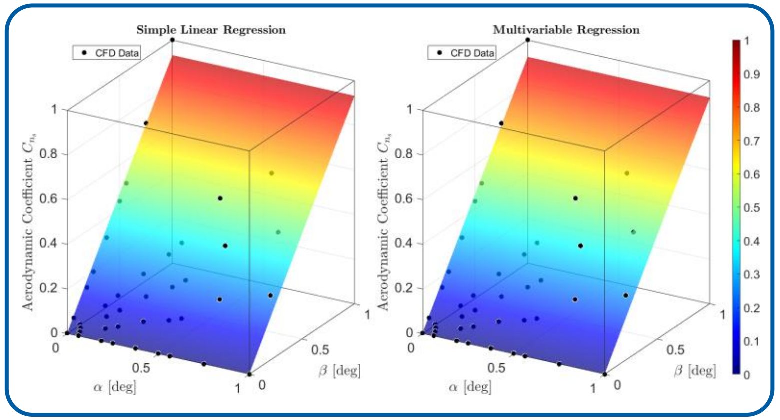

(e)

Figure 14. Interpolations results comparison between the Simple Linear Regression and the Multivariable Regression models:

- (a) longitudinal force,
- (b) lateral force,
- (c) vertical force,
- (d) pitch moment,
- (e) yaw moment.